Coping with stress: morphological changes in response to environmental stimuli in a fungal plant pathogen

Carolina Sardinha Francisco[1], Xin Ma[1], Maria Manuela Zwyssig[1], Bruce A. McDonald[1], Javier Palma-Guerrero[1*]

[1]Plant Pathology Group, Institute of Integrative Biology, ETH Zürich, 8092 Zürich, Switzerland

*Corresponding author

E-mail: javier.palma@usys.ethz.ch

Abstract

During their life cycles, pathogens have to adapt to many biotic and abiotic environmental stresses to maximize their overall fitness. Morphological transitions are one of the least understood of the many strategies employed by fungal plant pathogens to adapt to constantly changing environments, even though different morphotypes may play important biological roles. We characterized the responses of the wheat pathogen *Zymoseptoria tritici* to a series of environmental stresses in order to understand the effects of changing environments on fungal morphology and adaptation. We found that all tested stresses induced morphological changes, but different responses were found among four different strains. A transcription analysis showed that morphogenesis and virulence factors are co-regulated. We discovered that *Z. tritici* forms chlamydospores and demonstrated that these structures are better able to survive extreme cold, heat and drought than other cell types. We also show that blastospores (the “yeast-like” form of the pathogen typically found only in laboratory conditions) can form from germinated pycnidiospores on the surface of wheat leaves, suggesting that this morphotype can play an important role in the natural history of *Z. tritici*. Our findings illustrate how changing environmental conditions can affect cellular morphology and lead to the formation of new morphotypes, with each morphotype having a potential impact on both pathogen survival and disease epidemiology.

Introduction

Fungi occupy a wide range of niches that can impose different environmental constraints on their growth, reproduction and survival. In response, fungi evolved the ability to detect and respond to different environmental stimuli to maximize their fitness [1]. One of the strategies that fungi employ to cope with diverse biotic and abiotic stresses is to change their morphology [2–4]. For fungal pathogens, different morphotypes can play different roles during the host-pathogen interaction to optimize overall pathogen fitness. For example, hyphae can be the most appropriate morphology to cross physical barriers, colonize host tissue [2,5], and escape harmful environments generated by host defences [2,6] while yeast cells (or “yeast-like" cells) may be a better morphology to enable dispersal among host niches or between hosts and increase the pathogen population size [2,7]. The majority of fungal morphotype transitions occur between hyphal and yeast growth forms. Fungi with this ability are called dimorphic. Usually, they grow as saprophytic molds that live on dead organic matter and many are facultative human pathogens, though dimorphism is also found in plant pathogens [2,8,9]. The morphological transition can be co-regulated with the expression of genes encoding virulence [2–5,7,10,11]. The induction of virulence genes is usually associated with a specific morphotype. For example, certain virulence genes are expressed only during the yeast-phase of growth in *Histoplasma capsulatum,* while other virulence genes are expressed only during hyphal growth in *Candida albicans* [5,6,12].

65 Some fungi can produce additional morphologies, including pseudohyphae and
66 chlamydospores. Fungi that can produce more than two morphotypes are called
67 pleomorphic. Pseudohyphae are distinguished from true hyphae by constrictions that
68 form at the septal junctions, leading to a loss in cytoplasmic continuity between mother
69 and daughter cells [13]. Though little is known about the ecological significance of
70 pseudohyphae and their role during host infection, it was suggested that this
71 morphotype facilitates foraging for scarce nutrients and increases motility in the host
72 [7,14]. Chlamydospores are spherical, thick-walled cells formed on the tips of
73 pseudohyphae or on distal parts of differentiated hyphae called suspensor cells [15]. In
74 contrast to pseudohyphae, chlamydospores are well-characterized and known to
75 operate as long-term survival structures that can resist many environmental stresses
76 [15–19]. Pleomorphism has been observed in fungal pathogens of humans [15,17,20]
77 and plants [18,21,22].
78
79 *Zymoseptoria tritici* is the most damaging pathogen of wheat in Europe [23,24] and an
80 important pathogen of wheat worldwide. *Z. tritici* is considered a dimorphic fungus that
81 grows either as blastospores (the “yeast-like” form) or as filamentous hyphae depending
82 on the culture conditions. Though the role of blastospores in nature was unclear until
83 now, hyphae are essential for penetrating wheat leaves through stomata [25,26]. The
84 stimuli that induce morphological changes and the cell signaling pathways involved in
85 morphological transitions remain largely unknown in this pathogen. Nutrient-rich media
86 and temperatures ranging from 15°C to 18°C tend to induce blastosporulation
87 (blastospore replication by budding) while nutrient-limited media and high temperatures

88 (from 25°C to 28°C) tend to promote the blastospore-to-hyphae transition in the *Z. tritici*
89 reference strain IPO323 [27,28]. Some genes affecting morphogenesis in *Z. tritici* were
90 identified and functionally characterized. Most of these belonged to the mitogen-
91 activated protein kinase (MAPK) or cAMP-dependent signaling pathways involved in
92 extracellular signal transduction, regulating many cellular processes, development and
93 virulence [27–37]. However, the transcriptome signatures associated with specific
94 morphotypes were not reported until now.
95
96 In this study we aimed to characterize how environmental changes affect morphology and
97 adaptation in a fungal plant pathogen. We found that *Z. tritici* changed its morphology in
98 response to all tested stresses, though distinct responses were observed for four different
99 strains sampled from the same geographical population. Transcriptional analyses showed
100 a co-regulation of mycelial growth with expression of virulence factors. We discovered that
101 *Z. tritici* forms chlamydospores both *in vitro* and *in planta*. We also found that
102 pseudohyphae will form in some environments. We showed that blastospores can form
103 by budding from pycnidiospores inoculated onto the surface of wheat leaves,
104 demonstrating that blastospores can be produced under natural conditions. Based on
105 these findings, we propose that morphological transitions in *Z. tritici* are a stress response
106 that allows the fungus to optimize fitness in a changing environment.
107
108
109 **Results**

110 **High temperature induces different morphological responses among *Z. tritici***
111 **strains.**
112 We exposed four different *Z. tritici* strains growing in yeast sucrose broth (YSB) at 27°C,
113 a highly stressful temperature for *Z. tritici*. Three of the strains (1E4, 3D1, and 3D7)
114 differentiated to filamentous growth at 27°C (Fig 1) as previously reported for the
115 reference strain IPO323 [27,28]. The timing of the hyphal transition ranged from 8 hours
116 after incubation (hai) for 1E4, to 24 hai for 3D1 and 3D7 (Figs 1B and 1C). Branching
117 and hyphal elongation were frequently observed at 48 hai (Figs 1D-1F). Surprisingly,
118 high temperature promoted the formation of two new morphologies, with appearances
119 matching pseudohyphae and chlamydospores, in the 1A5 strain (Figs 1E and 1F).
120 However, no hyphal growth was observed for this strain. Interestingly, chlamydospore-
121 like cells were found for all strains at 144 hai (Fig 1F). Cellular differentiation from
122 blastospores to pseudohyphae began in 1A5 at 24 hai, resulting in a series of conjoined
123 elongated cells, characteristic of pseudohyphae [13] (Fig 1C). We also observed several
124 swollen cells at 24 hai that we believe represent the initial differentiation from
125 blastospores into chlamydospore-like cells (Fig 1C), but the complete differentiation
126 occurred between 48 and 96 hai (Figs 1D and 1E). Chlamydospore-like cells were
127 observed at the ends of pseudohyphae or distal parts of filamentous hyphae (Fig 1F).
128 Chlamydospore-like cells that were detached from suspensor cells were also found
129 (data not shown). Blastospores incubated in YSB at 18°C continued to replicate only as
130 blastospores via blastosporulation and were used as controls (Fig 1A).
131
132 **A nutrient-limited environment promotes filamentous growth.**

133 Carbon- or nitrogen-depleted medium promoted hyphal growth in all four strains (Fig 2;
134 S1 Fig). In a carbon-depleted environment (Minimal medium (MM) without sucrose),
135 cellular differentiation occurred after 24 hours of incubation (Fig 2). At 24 hai, hyphal
136 formation was observed with the first hyphal branch formed terminally (1A5 and 3D1) or
137 laterally (1E4 and 3D7) (Fig 2B). Hyphal elongation and branching continued at 48 and
138 72 hai (data not shown). By 144 hai mycelial growth was predominant, with frequent
139 anastomosis events among hyphae (Fig 2C). In MM with sucrose, all strains grew as a
140 mixture of blastospores and hyphae, with blastospores budding from filamentous hyphae,
141 showing that the morphological transition is bidirectional (S1C Fig). Blastospores
142 incubated in YSB continued to replicate only as blastospores via blastosporulation (Fig
143 2A).
144
145 In nitrogen-depleted media (MM without ammonium nitrate), three strains (1A5, 3D1, and
146 3D7) initially formed hyphae from one apical end, generating the first and second hyphal
147 elongations within 72 hai (S1B Fig). 1E4 responded most quickly to a low nitrogen
148 environment, with hyphae forming at 24 hai (S1A Fig) and a network of filamentous
149 hyphae formed at 72 hai (S1B Fig). In regular MM all strains grew as a mixture of
150 morphotypes (S1C Fig). Interestingly, the hyphae induced under both carbon and nitrogen
151 limitation (Fig 2; S1 Fig) were thinner than those produced by high temperature (Fig 1).
152
153 **Oxidative stress induces morphological changes in some strains**.
154 To determine the effect of oxidative stress on the *Z. tritici* morphology we examined the
155 growth in presence of hydrogen peroxide (H_2O_2) at two different spore concentrations. At

156 a high initial cell density (10^5 blastospores/mL), the presence of H_2O_2 stimulated hyphal
157 growth in 1E4 up to a concentration of 5 mM (S2 Fig). 1A5, 3D1, and 3D7 continued to
158 replicate as blastospores, but there was a substantial reduction in blastospore formation
159 starting at 5 mM H_2O_2 (S2 Fig). To test whether a lower concentration of blastospores
160 would change sensitivity to oxidative stress, we inoculated flasks with 10^3
161 blastospores/mL. After 72 hours of incubation in 0.5 mM H_2O_2, strains 1E4 and 3D1
162 showed apical and lateral hyphal branching (S3 Fig), but both strains continued to form
163 blastospores. At 1 mM, blastospores from 1E4, 3D1, and 3D7 developed into a mixture of
164 pseudohyphae and regular hyphae (S3 Fig). The higher sensitivity at low cell densities
165 suggests that the exogenous H_2O_2 was more rapidly degraded by secreted
166 hydroperoxidase proteins (catalases, peroxidases and catalase-peroxidase) when cell
167 densities were 100X higher. The 1A5 strain did not switch to a different morphotype at
168 any H_2O_2 concentration, continuing to replicate as blastospores (S3 Fig). Starting at 2 mM
169 H_2O_2, none of the strains changed their morphology (S3 Fig) and blastosporulation ceased
170 (from 5 mM to 10 mM), suggesting a cytotoxic effect of H_2O_2 at these concentrations.
171
172
173 **Inoculum size effect suggests that quorum sensing may affect morphology.**
174 In order to evaluate the effect of the inoculum size on the morphological transition, we
175 incubated all four strains at five cell densities in two growth conditions shown to induce
176 hyphal growth. After 144 hours of incubation in C-depleted medium, we observed that
177 morphology was independent of cell density for all four strains up to a concentration of
178 10^5 blastospores/mL (S4A Fig), with most of the blastospores switching to hyphal growth

179 and forming mycelial colonies. However, when the initial cell density was $\geq 10^6$
180 blastospores/mL, we observed a substantial reduction in the blastospore-to-hyphae
181 transition and in hyphal length. No hyphae formed for 3D1 and 3D7 at initial cell densities
182 of 10^7 blastospores/mL, and they were clearly reduced for 1E4 and 1A5 (S4A Fig).
183
184 In YSB at 27°C we also found that initial inoculum size affected cell morphology (S4B
185 Fig), though there were more pronounced differences among strains in this environment.
186 At 144 hai, starting from the lowest initial cell density (10^3 blastospores/mL), we
187 observed pseudohyphae formation in 1A5, 1E4, and 3D1, and a mixture of
188 pseudohyphae and chlamydospore-like cells in 3D7. At an initial density of 10^4
189 blastospores/mL, the same phenotypes were found, except that 3D1 formed apical and
190 lateral hyphae. Intermediate initial cell densities (10^5 and 10^6 blastospores/mL)
191 promoted hyphal growth for 1E4, 3D1 and 3D7, but the 3D7 strain grew as a mixture of
192 mycelium and chlamydospore-like cells at 10^6 blastospores/mL. The increase of the
193 inoculum size to 10^7 blastospores/mL induced formation of chlamydospore-like
194 structures in 1E4 and 3D1, and a transition from blastospores to pseudohyphae and
195 chlamydospore-like cells in 3D7. 1A5 was not able to switch to hyphae under high
196 temperatures in any of the initial cell densities (S4B Fig). The overall pattern of cell
197 density dependence shown here suggests that a quorum sensing molecule may be
198 controlling the morphological transition, as has been reported for other pleomorphic
199 fungi [38–40].
200

201 **Mycelial growth is co-regulated with virulence-related genes.**

202 Aiming to identify genes associated with mycelial growth in nutrient-poor environments,
203 we compared the transcriptomes from blastospores and two different hyphal inducing
204 conditions for the four strains (S5Fig). The total number of sequencing reads and mapped
205 reads per strain under different growth conditions is given in S1 Table. A total of 4888,
206 5296, 5323, and 6003 genes were differentially expressed among all tested conditions in
207 1A5, 1E4, 3D1, and 3D7, respectively. On average, 24% and 25% of the genes were
208 upregulated during blastospore and mycelial growth, respectively.

209

210 The upregulated genes shared among all four strains for each morphology were selected
211 based on pairwise comparisons. Two distinct sets of 134 genes shared among the four
212 strains were identified in both comparisons. The first set is composed of genes that were
213 upregulated during blastospore growth: these genes were upregulated in YSB compared
214 to C-depleted medium, and were upregulated in YSB compared to 7dpi infection, FDR
215 ≤0.01 (S6A Fig; S2 Table). The second set consists of genes that were upregulated during
216 mycelial growth: these were upregulated in C-depleted medium compared to YSB, and
217 were upregulated in wheat infection compared to YSB, FDR ≤0.01 (S6B Fig; S3 Table).
218 For both comparisons, the sets of genes that do not overlap represent genes with a strain-
219 specific expression profile.

220

221 Among the 134 shared genes that are significantly upregulated during blastospore growth,
222 20% are annotated as *hypothetical proteins* (Fig 3A; S2 Table). The remaining 107 genes

223 are divided into fourteen biological process categories, with *metabolism* being the most
224 represented term (44%). This category was composed mainly of non-secreted enzymes,
225 including oxidoreductases (n=11), dehydrogenases (n=8), hydrolases (n=7), and
226 transferases (n=9) (Fig 3A). No enrichment was found for any other category. However,
227 seven genes from other categories were already described in other fungi to be involved
228 in blastosporulation (S4 Table). As expected, genes related to vegetative blastospore
229 growth were highly expressed in nutrient-rich medium - the environment most conducive
230 for this morphotype (S6C Fig).
231
232 Among the 134 genes that were upregulated in all strains during mycelial growth, we
233 observed an enrichment of secreted proteins (32%) known to be associated with fungal
234 virulence, including *candidate effectors* (small secreted proteins - SSPs), *secreted*
235 *proteases*, *secreted glycosidases*, *secreted chloroperoxidases, cell wall hydrolases,*
236 *hydrophobins,* and *hydrophobic surface binding proteins* (Fig 3B; S3 Table). Overall,
237 these virulence-associated genes were upregulated in C-depleted medium and during
238 all stages of plant infection, albeit with a reduction in expression during the saprophytic
239 phase of infection (at 28 dpi). The peak of expression of these virulence-associated
240 genes preceded the first visual symptoms of infection, at 12 dpi for 1A5 and 3D7, and at
241 14 dpi for 1E4 and 3D1 (S6D Fig), as previously reported for some of these gene
242 categories [41]. These patterns suggest that mycelial growth is co-regulated with the
243 expression of genes relevant for virulence even in the absence of the host. We also
244 detected the upregulation of six genes related to cellular morphogenesis (S5 Table). The
245 transcription profiles of these genes showed an upregulation in both mycelial growth

246 conditions (C-depleted medium and plant infection at 7 dpi) with the peak of expression
247 occurring at 7 dpi for all four strains (S6E Fig).
248
249 **Chlamydospore-like cells are produced by *Z. tritici*.**
250 As mentioned above, we observed the formation of structures with the same
251 morphology as chlamydospores. These structures had never been previously reported
252 in *Z. tritici*. We aimed to determine whether these chlamydospore-like cells had
253 properties associated with chlamydospores in other fungi. Chlamydospores are known
254 to be survival structures that have thicker cell walls and a high content of lipid droplets
255 [42]. We stained the different morphological cell types of 1A5 with the chitin-binding dye
256 Calcofluor White (CFW) and the lipid droplets dye Nile Red (NR) to measure these
257 properties. The intensity of CFW fluorescence was higher in chlamydospore-like cells
258 (Fig 4A-4C) compared with blastospores, hyphae, and pseudohyphae that exhibited a
259 weaker fluorescence for CFW (Fig 4). NR staining revealed that chlamydospore-like
260 cells had a high content of lipid droplets, which was also observed for blastospores and
261 pseudohyphae. On the contrary, hyphae showed a lower lipid droplet content than
262 spores, with the exception of the hyphal branching zones (Fig 4) as has been reported
263 for other fungi [43]. We then examined the thickness of the cell walls for three cell types
264 using transmission electron microcopy (TEM). TEM showed that the chlamydospore-like
265 cells had thicker cell walls than blastospores and pycnidiospores (Fig 5). We also found
266 that pseudohyphae and the elongated suspensor cells, where chlamydospores are
267 usually attached to the surrounding mycelium, have a cell wall thickness similar to
268 pycnidiospores (Fig 5). No differences were observed for the chlamydospore-like cells

269 produced by the 1A5 and 3D7 strains. On average, chlamydospore-like cells produced
270 by *Z. tritici* had a cell wall thickness of ~460 nm, about four times thicker than the cell
271 walls found in blastospores and pycnidiospores. Despite the thickness of the cell wall,
272 we could not differentiate an extra cell wall layer as reported in chlamydospores from
273 other fungal species [44,45].
274
275 To determine if the chlamydospore-like cells are also produced during plant infection,
276 wheat plants were inoculated with pycnidiospores of all four strains expressing
277 cytoplasmic GFP and kept in a greenhouse chamber until pycnidia formation. Microscopic
278 examination of the spore solution harvested from 20-day old infected leaves showed the
279 presence of chlamydospore-like cells mixed among the pycnidiospores (S7 Fig).
280
281
282 **The chlamydospore-like cells are metabolically active and highly stress tolerant.**
283 The chlamydospore-like cells of 1A5 germinated and produced hyphae. After 12 hours of
284 incubation on water agar (WA) plates, we observed germ tubes emerging from the
285 chlamydospore-like cells, which led to the development of hyphae at 24 hai (Fig 6B and
286 6C). Blastospores used as controls initially germinated from one apical side, generating
287 the first and second germ tubes within 12 hai (Fig 6A). We inoculated wheat with
288 chlamydospore-like cells from GFP-tagged 1A5 to observe by confocal microscopy
289 whether these cells could germinate on the leaf surface. At 24 hpi, free chlamydospore-
290 like cells and chlamydospore-like cells still attached to a suspensor cell produced germ

291 tubes and hyphae on the surface of wheat leaves (Fig 6D). These results suggest that
292 chlamydospore-like cells may be able to cause infections.
293
294 We also investigated whether chlamydospore-like cells share other characteristics of
295 fungal resting spores, such as an ability to resist drought and temperature extremes.
296 Incubation for one day under drought stress reduced viability of blastospores and
297 pseudohyphae by 70%, while the chlamydospore-like cells had a reduction in cell viability
298 of only 23% (Fig 7A). These rates changed little after 3 days of drought stress. After 5
299 days of drought stress, the survival rates were 10%, 19%, and 49% for blastospores,
300 pseudohyphae and chlamydospore-like cells, respectively (Fig 7A). After 10 days of
301 drought stress, the chlamydospore-like cells exhibited a survival rate of 50%, significantly
302 higher than the other cell types (Fig 7A). In the cold stress experiment, only the
303 chlamydospore-like cells survived the cold shock, with no statistically significant difference
304 in the survival rates of 23%, 17%, and 19% after 1 min, 2 min and 3 min in liquid nitrogen,
305 respectively (Fig 7B). In the heat stress experiment, 30°C affected blastospores and
306 chlamydospore-like cells equally, but the 35°C treatment killed all the blastospores while
307 chlamydospore-like cells and pseudohyphae survived at rates of 12% and 6%,
308 respectively (Fig 7C). None of the morphotypes survived at 40°C (Fig 7C). For all tested
309 environmental stresses, chlamydospore-like cells were the morphotype that exhibited the
310 highest survival rate, suggesting that this structure exhibits ecological characteristics
311 typical for fungal resting spores that enable improved survival to different stresses
312 encountered in nature.
313

314

315 **Germinating pycnidiospores produce blastospores on the surface of wheat leaves.**
316 Pycnidiospores of a GFP-tagged 3D7 strain were inoculated onto wheat plants and
317 monitored using confocal microscopy. At 24 hai, we observed the expected pycnidiospore
318 germination and initial hyphal branching, but we also observed newly-budding
319 blastospores (Fig 8A). After 48 hours, there was an increase in the number of budding
320 points on germinated pycnidiospores, and an increase in the number of free blastospores
321 visible on the leaf (Fig 8B). This suggests that pycnidiospores of *Z. tritici* can germinate to
322 produce additional blastospores even before penetration of the wheat leaf, providing an
323 alternative mechanism for splash-dispersal of infective propagules and potentially
324 providing a substantial increase in the total inoculum load associated with an infection
325 cycle. At 48 hpi we also noticed many anastomosis events between pycnidiospores and
326 new blastospores (Fig 8B).

327

328 ## Discussion

329 Fungi evolved to perceive a wide array of environmental signals and reprogram their
330 cellular responses accordingly in order to maximize their fitness. Though much research
331 has been oriented around morphological changes and their associated transcriptional
332 pathways in response to different stressors in fungal pathogens of humans [10,15,46],
333 knowledge in this area is limited for plant pathogens. Our study shows how different
334 environmental stresses can affect cellular morphologies in the wheat pathogen *Z. tritici*.
335 We also demonstrate the phenotypic plasticity of this fungus in response to

336 environmental changes, as well as differential responses to the same environments
337 among strains. An unexpected outcome of this study was the discovery of two novel
338 morphotypes, one of which may have important epidemiological consequences.
339
340 We found that several environmental stresses can affect morphological transitions in
341 strain-specific ways for four natural *Z. tritici* strains sampled from the same Swiss
342 population. All four strains switched to hyphal growth in a nutrient-poor minimal medium.
343 Morphological changes induced by limited nutrients have also been described in other
344 dimorphic plant pathogenic fungi distributed across different phyla [9,47]. Nutrients are
345 known to be present on the leaf surface in very small quantities and are usually
346 surrounded by epicuticular waxes [48]. As a result, plant pathogens typically experience
347 nutritient limitations while growing on leaves. It is thought that secreted enzymes,
348 including plant cell wall degrading enzymes (PCWDEs) such as cutinases, are required
349 to obtain nutrients during this stage of development, but *Z. tritici* has few PCWDEs
350 compared to other fungi [49], suggesting that the perception of a nutrient-limited
351 environment may act as a stimulus to induce a switch to an exploratory morphotype
352 (hyphae) that can better explore the environment for food. We found a significant
353 increase in the frequency of anastomosis events during mycelium formation under
354 nutrient-limited conditions. Mycelial networks formed by anastomosis enable a shared
355 cytoplasmic flow that can more efficiently distribute water, nutrients, and signals within a
356 fungal colony [50,51]. Moreover, hyphal fusions were shown to be required for virulence
357 for some plant pathogens [52,53]. We hypothesize that hyphal anastomosis provides
358 benefits during epiphytic growth of germinating *Z. tritici* pycnidiospores prior to stomatal

359 penetration, with anastomosis facilitating colony establishment and increasing strain
360 fitness during colonization of the host.
361
362 The oxidative burst is a ubiquitous plant defense response to pathogen infection,
363 resulting in a rapid release of reactive oxygen species (ROS), including hydrogen
364 peroxide (H_2O_2) [54]. The ROS produced during plant defense were proposed to have
365 various functions, including activation of plant defense-related genes and production of
366 phytoalexins in addition to a direct antimicrobial effect that inhibits pathogen growth [55–
367 57]. Though many studies have demonstrated its antimicrobial effects, the effects of
368 H_2O_2 on morphological transitions remain largely unexplored. In *Candida albicans*, H_2O_2
369 induces hyphal differentiation in a dose-dependent manner [58]. Our results show that
370 blastospores of three out of four *Z. tritici* strains switch to hyphae and pseudohyphae
371 when exposed to H_2O_2 in a dose-dependent manner. A cell density dependence was
372 also found. The different cell density responses suggest that the H_2O_2 is more rapidly
373 metabolized by fungal hydroperoxidase proteins (catalases, peroxidases and catalase-
374 peroxidase), leading to lower toxicity at higher cell densities. Several genes encoding
375 peroxidases and catalase-peroxidases were identified in the genome of *Z. tritici* [59,60],
376 which may explain the observed phenotype. The inability of 1A5 to differentiate hyphae
377 from blastospores at any H_2O_2 concentration suggests that this strain either cannot
378 sense oxidative stress or that it possesses a more efficient antioxidant response that
379 can neutralize the effects of H_2O_2. Further experiments will be needed to test these
380 hypotheses.
381

382 Temperature is an important abiotic factor that strongly affects growth, reproduction, and
383 development in fungi [66,67]. Thermally dimorphic human fungal pathogens usually
384 undergo morphological transitions in response to host temperature [47,68]. *Z. tritici* is the
385 first plant pathogen shown to undergo morphological transitions after exposure to high
386 temperatures [28,66]. Our experiments showed that a change in temperature from 18°C
387 to 27°C triggered hyphal growth in three out of four tested *Z. tritici* strains. For these
388 three strains, an increase in hyphal elongation and formation of branches occured soon
389 after exposure to the higher temperature. The hyphae formed at a high temperature
390 appeared thicker than those formed under nutritient limitations and it is not clear if they
391 would be able to cause infections.
392
393 We used transcriptome sequencing to identify genes associated with mycelial growth in
394 *Z. tritici*. It was shown in other plant pathogenic fungi that starvation induces the
395 expression of virulence-related genes [69,70]. In *Z. tritici*, we found that genes relevant
396 for virulence, including secreted hydrolytic proteins and candidate effectors, were
397 upregulated in both hyphae-inducing conditions (carbon-depleted medium and *in*
398 *planta*), suggesting that genes controlling morphogenesis and virulence may be co-
399 regulated under nutrient-limited conditions. In *C. albicans,* genes related to hyphal
400 growth are co-regulated by transcription factors that affect expression of genes involved
401 in virulence [5,7]. However, it is important to note that not every virulence function is
402 connected to morphogenesis. The specific genes involved in the activation and
403 regulation of these morphological transitions remain unknown for *Z. tritici*.
404

405 An unexpected outcome of this study was the discovery of chlamydospore-like cells in *Z.*
406 *tritici.* The preponderance of evidence indicates that these cells are truly
407 chlamydospores. Their morphology matched the chlamydospores described in other
408 fungi: spherical, thick-walled cells with a high lipid content that form either intercalated or
409 at the ends of filamentous hyphae and occasionally on pseudohyphae [17,71]. We also
410 showed that these cells were able to survive several stresses that killed other cell types,
411 including dessication and high and low temperatures, consistent with the function of
412 chlamydospores as long-term survival structures in other fungi [16–18,72]. We conclude
413 that *Z. tritici* produces chlamydospores.
414
415 This is the first time that chlamydospores have been found in a plant pathogen that is
416 thought to mainly inhabit the phyllosphere. Though chlamydospores were especially
417 prominent in the 1A5 strain at high temperature, we observed chlamydospore production
418 in all four strains both *in vitro* and *in planta*. We hypothesize that the chlamydospores
419 produced by *Z. tritici* may contribute an important source of inoculum that can survive
420 between growing seasons and perhaps form a long-term spore-bank that can persist for
421 many years in wheat-growing regions. Chlamydospores may also contribute to long-
422 distance movement of the pathogen on infested straw or seeds. These properties could
423 impact the management of septoria tritici blotch (STB), but additional studies will be
424 needed to understand the roles played by chlamydospores during the STB disease cycle.
425
426 Another finding with epidemiological implications was to demonstrate that blastospores
427 can form from germinating pycnidiospores on the surface of wheat leaves. This

428 possibility was proposed more than 30 years ago [73,74], but was not followed up in
429 subsequent studies. The formation of blastospores during *in vitro* growth in nutrient-rich
430 medium is why *Z. tritici* has long been considered to be a dimorphic fungus, but until
431 now it was not clear if the blastospores could also form on leaf surfaces in nature. Our
432 experiments confirmed that blastospores are produced during a natural infection. It
433 remains unclear whether blastospores make a significant contribution to the
434 development of epidemics. Given their small size and increasing abundance over time,
435 we hypothesize that they may play an important role in the explosive increase in STB
436 that can occur following prolonged rainy periods that last for several days [73,75].
437
438 In conclusion, we demonstrate that a fungal plant pathogen responds morphologically to
439 diverse environmental stresses, and we propose distinct biological roles for different
440 morphotypes. We also illustrate the advantage of including different natural strains when
441 studying the response of a species to environmental stresses, as we found different
442 morphological responses among the tested strains. Our findings provide important new
443 insights into the *Z. tritici*-wheat pathosystem including: 1) the phenotypic plasticity of *Z.*
444 *tritici* in response to different environmental changes; 2) the reclassification of *Z. tritici* as
445 a pleomorphic fungus due to its ability to produce four distinct morphotypes; 3) the
446 discovery of chlamydospores that may help the fungus to survive stressful conditions; 4)
447 the formation of blastospores from germinating pycnidiospores on the surface of wheat
448 leaves, enabling a potentially significant increase in inoculum size. These findings position
449 *Z. tritici* as an excellent model organism to explore how morphological changes can affect
450 adaptation to different environments in fungal plant pathogens.

451

452 ## Materials and methods

453 **Fungal strains, environmental stimuli, and growth conditions.**

454 Four previously characterized *Zymoseptoria tritici* strains (ST99CH_1A5, ST99CH_1E4,
455 ST99CH_3D1, and ST99CH_3D7, abbreviated as 1A5, 1E4, 3D1, and 3D7,
456 respectively); [76,77], were used in this study. Strains expressing cytoplasmic GFP [78]
457 were provided by Andrea Sanchez-Vallet after being generated by Sreedhar Kilaru and
458 Gero Steinberg as described in Zala *et al* 2018 [79]. All strains were grown in YSB
459 (yeast extract 10 g/L and sucrose 10 g/L; pH 6.8). Depending on the tested
460 environment, we used either YSB or a defined salts medium (Minimal Medium – MM, pH
461 5.8; [80]. Each strain was stored in glycerol at -80°C until required and then recovered in
462 YSB medium incubated at 18°C for three days. For nutrient limitation experiments, the
463 cells were washed three times with sterile distilled water to remove any remaining
464 nutrients prior to placing them into nutrient-limited conditions. Cell concentrations were
465 determined by counting blastospores using a KOVA cell chamber system (KOVA
466 International Inc., USA).

467

468 **Effect of temperature on growth morphology.**

469 Blastospores of each strain were inoculated on YSB at a final concentration of 10^5
470 blastospores/mL. Three flasks were incubated at 18°C (as control) and three at 27°C for
471 four days. An aliquot was taken from each flask at 8, 24, 48, 96, and 144 hai to monitor
472 cell morphology by light microscopy using a Leica DM2500 microscope with LAS version
473 4.6.0 software. These experiments were repeated three times.

474

475 **Effect of nutrient limitation on growth morphology**.

476 MM was used to monitor the transition in growth morphologies under different nutrient
477 limitations. The effect of carbon depletion was assessed by adding each strain at a final
478 concentration of 10^5 blastospores/mL into either regular MM, which contains sucrose as
479 the main carbon source, or into MM without sucrose (C-depleted medium) and incubated
480 at 18°C. The cell morphology was observed by light microcopy every 24 hours until 144
481 hai. The effect of nitrogen depletion was determined using MM lacking ammonium nitrate,
482 which is normally present in MM as the main nitrogen source. We compared the growth
483 morphologies of cells growing in MM with and without ammonium nitrate by light
484 microcopy during 96 hours of incubation at 18°C. The growth morphologies in both
485 nutrient-limited conditions were compared to the morphologies found in the nutrient-rich
486 YSB. Experiments were repeated three times for each nutrient environment.

487

488 **Effect of oxidative stress on growth morphology.**

489 H_2O_2 was added into YSB at different concentrations (0, 0.5, 1, 2, 5, and 10 mM) to induce
490 different levels of exogenous oxidative stress. Each strain was added to a final
491 concentration of 10^5 blastospores/mL and incubated at 18°C. Morphological changes and
492 cellular morphologies were observed by light microscopy at 72 hai. To determine whether
493 a lower concentration of blastospores promotes a higher susceptibility to oxidative stress,
494 we performed the same experiment using a final concentration of 10^3 blastospores/mL.
495 These experiments were repeated twice.

496

497

498 **Effect of inoculum size on growth morphology.**

499 Flasks containing YSB or C-depleted medium were inoculated with a final cell density of
500 10^7 blastospores/mL, followed by a 10X serial dilution to a concentration of 10^3
501 blastospores/mL. Flasks containing C-depleted medium were incubated at 18°C and
502 flasks with YSB were incubated at 27°C. Cell morphology was determined every 24 hours
503 using light microscopy over 144 hours of incubation. These experiments were repeated
504 three times.

505

506 **RNA extraction, library preparation, and sequencing**.

507 Flasks containing a final concentration of 10^5 blastospores/mL in YSB or C-depleted
508 medium were incubated at 18°C to induce blastosporulation or mycelial growth,
509 respectively. Total RNA was extracted by using TRIzol (Thermo Fisher Scientific,
510 Waltham, Massachusetts) following the manufacturer's instructions. RNA quality was
511 checked using a Qubit fluorometer (Thermo Fisher Scientific, Waltham, Massachusetts)
512 and a TapeStation 2200 (Agilent, Santa Clara, California). Truseq stranded mRNA kit
513 (Illumina Inc., San Diego, CA, USA) was used for library preparation, and ribosomal RNA
514 was depleted by polyA enrichment. The quality and quantity of the enriched libraries were
515 assessed using a Qubit fluorometer (Thermo Fisher Scientific) and TapeStation (Agilent).
516 Libraries were sequenced on the Illumina HiSeq 2500 at 4 x 100 bp paired end reads.

517

518 **Transcriptome mapping and quantification.**

519 The sequencing adapters and reads shorter than 15 bp were trimmed from raw Illumina
520 reads using Trimmomatic v.0.36 [81] with the following settings:
521 ILLUMINACLIP:TrueSeq3-PE.fa:2:30:10, LEADING:2 TRAILING:2,
522 SLIDINGWINDOW:4:15 MINLEN:15. Filtered reads of each *Z. tritici* strain for the most
523 common growth morphologies (blastospores and mycelial growth) were mapped against
524 their respective genomes using Tophat v.2.0.13 [82]. HTSeq-count v.0.6.1 was used to
525 calculate the gene counts [83]. Mapped reads with more than one reported alignment
526 were excluded from further analyses. We applied the TMM (trimmed mean of M values)
527 method implemented in the Bioconductor edgeR v.3.12.0 package to normalize the
528 gene counts and to calculate the differentially expressed genes under each condition
529 [84,85]. Only genes with average counts per million reads per sample >1 for at least one
530 growth condition were counted as expressed genes. The Benjamin-Hochberg false
531 discovery rate (FDR) correction was used to adjust p-values based on the Fisher exact
532 test.
533
534 **Transcription profile analysis**.
535 We generated the CPM (counts per million mapped reads) values based on TMM-
536 normalized library sizes obtained from the edgeR v.3.12.0 package [84]. Only genes
537 with adjusted p-values of FDR≤0.01 were included in the analysis. The published
538 transcriptomes of each strain during wheat infection at 7 dpi [41] were used for
539 comparative analyses (datasets in NCBI SRA SRP077418). Only genes that were
540 significantly upregulated during both wheat infection at 7 dpi and in C-depleted medium

541 compared to YSB were considered to be mycelial growth-related genes. These genes
542 were used in further analyses. Specific transcriptome signatures were identified based
543 on the differentially expressed genes that were shared among all four strains under each
544 growth condition, according to the *Z. tritici* reference genome annotations [86,87]. We
545 also used the published transcriptomes of different stages of wheat infection [41] to
546 interpret the expression profiles of some genes under both axenic and *in planta*
547 conditions. The $\log_2$-transformed CPM values of those genes were plotted using the R
548 package ggplot2 [88].
549
550 **Fluorescence microscopy to quantify chitin and lipids in different morphotypes.**
551 Blastospores of 1A5 were inoculated into YSB to a final concentration of 10^5
552 blastospores/mL and incubated at 18°C or 27°C to induce blastosporulation or
553 chlamydospore-like formation, respectively. 1A5 was also inoculated at the same
554 concentration into C-depleted medium and incubated at 18°C to induce hyphal growth.
555 After four days of incubation, the resulting cells were harvested and fixed with 70% (v/v)
556 ethanol for 30 minutes, followed by three washes with phosphate buffer saline (PBS). The
557 cells were stained with 1 μg/mL of CFW and 2.5 μg/mL of NR (both reagents from Sigma-
558 Aldrich Chemie Gmbh, Munich, Germany) for 15 minutes. The stained cells were viewed
559 with a Leica DM2500 fluorescence microscope with LAS version 4.6.0 software, using a
560 UV filter system for CFW consisting of a BP excitation filter at 340-380 nm and a long
561 pass emission filter (>425 nm), and a red filter system for NR consisting of a BP excitation
562 filter at 546/10 nm and an emission filter at 585/40 nm.

563

564 **Transmission electron microscopy.**

565 Cells of 1A5 and 3D7 were collected after 4 days of growth in YSB at 18°C or 27°C.
566 Pycnidiospores for each strain were harvested from infected wheat plants. Samples were
567 prepared using microwave-assisted fixation in 0.1 M cacodylate buffer (2.5%
568 glutaraldehyde and 2% paraformaldehyde), using a PELCO Biowave (Ted Pella,
569 California, USA), followed by embedding in 2% low melting temperature agarose
570 (SeaPlaque Agarose, FMC Corporation, USA). A second step of microwave-assisted
571 fixation was used after embedding in agarose. Before resin infiltration, the samples went
572 through two steps of post-fixation, first in osmium tetroxide (OsO4) in 0.1 M cacodylate
573 buffer and then in 1% uranyl acetate (UrAc), followed by a graded series of ethanol
574 washes for dehydration (25%, 50%, 75%, 90%, and 100%). Samples were infiltrated with
575 Spurr resin and polymerized at 60°C for 48 hours. Ultrathin sections (60 nm) were cut
576 using the Leica Ultracut FC6 (Leica Microsystem, Vienna) and then transferred to formvar
577 coated carbon grids, followed by post-staining with uranyl acetate and lead citrate.
578 Micrographs were collected using a Morgagni 268 transmission electron microscope
579 operating at 100 kV and using a CCD (1376x1032 pixel) camera.

580

581 **Germination of chlamydospore-like cells and their survival under stress.**

582 Chlamydospore-like cells and blastospores of the 1A5 strain were harvested from YSB
583 after 4 days of growth at 27°C or 18°C, respectively, and their concentrations were
584 adjusted to ~10^5 cells/mL. 10 μL was spotted onto WA (1% agar in water) and the plates

585 were incubated at 18°C. Germ tube formation was checked at 0, 12, and 24 hours after
586 inoculation by light microscopy.
587
588 To determine whether chlamydospore-like cells differ in their ability to survive
589 environmental stresses compared to blastospores and pseudohyphae, we exposed $8x10^3$
590 cells/mL of each morphotype to different stresses, including drought and extreme
591 temperatures.
592
593 For drought stress, 200 μL of each cell solution were spread onto Amersham Hybond™
594 N^+ nylon membranes (GE Healthcare Life Sciences, Chicago, Illinois) and dried in a sterile
595 Petri dish placed on a sterile bench in a laminar flow hood. The Petri dishes were then
596 placed into a sealed box containing anhydrous silica gel for 1, 3, 5, or 10 days. After the
597 drought stress, the membranes were placed onto YMA plates (4g/L yeast extract, 4g/L
598 malt extract, 4g/L sucrose, and 12g/L agar), incubated at 18°C and colony formation was
599 monitored. Control membranes containing each morphotype were transferred directly to
600 YMA plates without any drying treatments.
601
602 For cold stress, 300 μL aliquots of each cell solution were submerged into liquid nitrogen
603 for 1, 2, or 3 minutes, and 200 μL of the thawed cell solution were spread onto YMA plates.
604 Control samples were incubated at room temperature. For heat stress, 200 μL aliquots of
605 each morphotype were incubated for 24 hours at 30, 35, or 40°C, followed by plating on
606 YMA. Controls were kept at 18°C. YMA plates from control and treated samples were

607 incubated at 18°C for seven days. Survival rates for each cell type were estimated based
608 on the number of colonies formed after exposure to the stressful conditions compared to
609 the number of colonies formed by the controls.
610
611 **Plant infection assays.**
612 The susceptible wheat cultivar Drifter was used in all experiments. Plant growth
613 conditions were described earlier [89]. All infection assays used 16-day-old plants. For
614 all four strains, blastospore suspensions produced after 3 days of growth in YSB at 18°C
615 were filtered through two layers of cheesecloth and diluted to a final concentration of 10^6
616 blastospores/mL in 30 mL of sterile water supplemented with 0.1% (v/v) Tween 20.
617 Spore suspensions were applied to run-off using a sprayer and the plants were kept for
618 three days in sealed plastic bags, followed by 21 days in a greenhouse. Leaves with
619 pycnidia were harvested and transferred to a 50 ml Falcon tube containing sterile water
620 and gently agitated to harvest the pycnidiospores. Pycnidiospore suspensions were
621 adjusted to a final concentration of 10^6 pycnidiospores/mL and a new batch of plants
622 were inoculated as described above. The plants infected by pycnidiospores were used
623 to observe the formation of chlamydospore-like cells on wheat plants.
624
625 To determine whether chlamydospore-like cells produce germ tubes and initiate hyphal
626 growth after coming into contact with the host, we inoculated Drifter with chlamydospore-
627 like cells from the 1A5 strain tagged with cytoplasmic GFP. Production of chlamydospore-
628 like cells was induced using high temperature (YSB at 27°C) as described above. The
629 suspension of chlamydospore-like cells was prepared and concentrations were

630 standardized as described for blastospore infections. The inoculation procedure was the
631 same except the inoculated plants were kept in plastic bags for only 24 hours.
632
633 To observe formation of chlamydospore-like cells *in planta*, infected leaves from wheat
634 plants inoculated with pycnidiospores were harvested at 20 dpi. The infected leaves were
635 incubated in a humidity chamber for 24 hours, following by washes with sterile distilled
636 water to collect the released spores. The spore suspension was checked for the presence
637 of chlamydospore-like cells using the fluorescent microcope with a GFP filter consisting
638 of a BP excitation filter at 480/40 nm and a BP emission filter at 527/30 nm.
639
640 To observe blastospore formation on the surface of wheat leaves, we inoculated plants
641 using blastospores of the 3D7 strain tagged with cytoplasmic GFP. At 21 dpi, GFP-tagged
642 3D7 pycnidiospores were harvested and a new batch of plants was inoculated using these
643 pycnidiospores as described earlier. The inoculated plants were kept in plastic bags at
644 100% humidity until they were examined for blastospores at 24 and 48 hai.
645
646 **Confocal microscopy of germinated pycnidiospores and chlamydospore-like cells.**
647 Confocal images were obtained using a Zeiss LSM 780 inverted microscope with ZEN
648 Black 2012 software. An argon laser at 500 nm was used to excite GFP fluorescence and
649 chloroplast autofluorescence with an emission wavelength of 490-535 nm and 624-682
650 nm, respectively. Plants inoculated with GFP-tagged 1A5 chlamydospore-like cells were
651 checked at 24 hai to observe germination of the chlamydospore-like cells. The same
652 confocal settings were used to determine whether pycnidiospores produced blastospores

653 on the leaf surface. Wheat plants inoculated with GFP-tagged 3D7 pycnidiospores were
654 checked at 24 and 48 hai.
655

656 ## Acknowledgements

657 We acknowledge Gero Steinberg and Sreedhar Kilaru for generating the fluorescent *Z.*
658 *tritici* Swiss strains used in this study, and Andrea Sanchez-Vallet for providing the strains.
659 We thank Daniel Croll and Andrea Sanchez-Vallet for critical reading of the manuscript.
660 We also thank Andrea Sanchez-Vallet, Lukas Meile, Julien P. L. Alassimone, and Danilo
661 A. Pereira for discussions in the course of this work. RNA processing and sequencing
662 were performed in the Genetic Diversity Center (GDC) of ETH Zurich and the Genomics
663 Facility of ETH Basel, respectively. Transmission electron microscopy (TEM) and confocal
664 microscopy were performed at the Scientific Center for Optical and Electron Microscopy
665 (ScopeM) of ETH Zurich.
666
667

668 ## References

669

670 1. Brown AJP, Cowen LE, di Pietro A, Quinn J. Stress Adaptation. Microbiology
671 Spectrum. 2017;5. doi:10.1128/microbiolspec.funk-0048-2016
672

673 2. Lin X, Alspaugh AJ, Liu H, Harris S. Fungal morphogenesis. Cold Spring Harbor
674 perspectives in medicine. 2014;5: a019679. doi:10.1101/cshperspect.a019679

675

676 3. Mayer FL, Wilson D, Hube B. *Candida albicans* pathogenicity mechanisms. Virulence.
677 2013;4: 119–128. doi:10.4161/viru.22913
678

679 4. Wang L, Lin X. Morphogenesis in fungal pathogenicity: shape, size, and surface.
680 PLoS Pathogens. 2012;8: e1003027. doi:10.1371/journal.ppat.1003027
681

682 5. Kumamoto CA, Vinces MD. Contributions of hyphae and hypha- co- regulated genes
683 to *Candida albicans* virulence. Cellular Microbiology. 2005;7: 1546–1554.
684 doi:10.1111/j.1462-5822.2005.00616.x
685

686 6. Brand A. Hyphal growth in human fungal pathogens and its role in virulence.
687 International Journal of Microbiology. 2012;2012: 517529. doi:10.1155/2012/517529
688

689 7. Thompson DS, Carlisle PL, Kadosh D. Coevolution of morphology and virulence in
690 *Candida* species. Eukaryotic Cell. 2011;10: 1173–1182. doi:10.1128/ec.05085-11
691

692 8. Lübbehüsen TL, Nielsen J, McIntyre M. Morphology and physiology of the dimorphic
693 fungus *Mucor circinelloides* (syn. *M. racemosus*) during anaerobic growth. Mycological
694 Research. 2003;107: 223–230. doi:10.1017/s0953756203007299
695

696 9. Nadal M, García- Pedrajas MD, Gold SE. Dimorphism in fungal plant pathogens.

697 FEMS Microbiology Letters. 2008;284: 127–134. doi:10.1111/j.1574-6968.2008.01173.x
698
699 10. Klein BS, Tebbets B. Dimorphism and virulence in fungi. Current Opinion in
700 Microbiology. 2007;10: 314–319. doi:10.1016/j.mib.2007.04.002
701
702 11. Nigg M, Laroche J, Landry CR, Bernier L. RNAseq analysis highlights specific
703 transcriptome signatures of yeast and mycelial growth phases in the Dutch Elm disease
704 fungus *Ophiostoma* novo-*ulmi*. G3: Genes|Genomes|Genetics. 2015;5: 2487–2495.
705 doi:10.1534/g3.115.021022
706
707 12. Edwards JA, Chen C, Kemski MM, Hu J, Mitchell TK, Rappleye CA. *Histoplasma*
708 yeast and mycelial transcriptomes reveal pathogenic-phase and lineage-specific gene
709 expression profiles. BMC Genomics. 2013;14: 1–19. doi:10.1186/1471-2164-14-695
710
711 13. Veses V, Gow NA. Pseudohypha budding patterns of *Candida albicans*. Medical
712 Mycology. 2009;47: 268–75. doi:10.1080/13693780802245474
713
714 14. Gancedo JM. Control of pseudohyphae formation in *Saccharomyces cerevisiae*.
715 FEMS Microbiology Reviews. 2001;25: 107–123. doi:10.1111/j.1574-
716 976.2001.tb00573.x
717
718
719

720 15. Noble SM, Gianetti BA, Witchley JN. *Candida albicans* cell-type switching and
721 functional plasticity in the mammalian host. Nature Reviews Microbiology. 2017;15: 96–
722 108. doi:10.1038/nrmicro.2016.157
723
724 16. Couteaudier Y, Alabouvette C. Survival and inoculum potential of conidia and
725 chlamydospores of *Fusarium oxysporum* f.sp. *lini* in soil. Canadian Journal of
726 Microbiology. 1990;36: 551–556. doi:10.1139/m90-096
727
728 17. Lin X, Heitman J. Chlamydospore formation during hyphal growth in *Cryptococcus*
729 *neoformans*. Eukaryotic Cell. 2005;4: 1746–54. doi:10.1128/EC.4.10.1746-1754.2005
730
731 18. McNeel DJ, Kulkarni RK, Nickerson KW. Pleomorphism in *Ceratocystis ulmi*:
732 chlamydospore formation. Canadian Journal of Botany. 1983;61: 1349–1352.
733 doi:10.1139/b83-143
734
735 19. Son H, Lee J, Lee YW. Mannitol induces the conversion of conidia to
736 chlamydospore-like structures that confer enhanced tolerance to heat, drought, and UV
737 in *Gibberella zeae*. Microbiological Research. 2012;167: 608–615.
738 doi:10.1016/j.micres.2012.04.001
739
740 20. Miyaji M, Sano A, Sharmin S, Kamei K, Nishimura K. The role of chlamydospores of
741 *Paracoccidioides brasiliensis*. Nippon Ishinkin Gakkai Zasshi. 2003;44: 133–138.
742 doi:10.3314/jjmm.44.133

743

744 21. Hoes JA. Development of chlamydospore in *Verticillium nigrescens* and *Verticillium*
745 *nubilum*. Canadian Journal of Botany. 1971;49: 1836–1866. doi:10.1139/b71-263
746

747 22. Schade D, Walther A, Wendland J. The development of a transformation system for
748 the dimorphic plant pathogen *Holleya sinecauda* based on Ashbya gossypii DNA
749 elements. Fungal Genetics and Biology. 2003;40: 65–71. doi:10.1016/s1087-
750 1845(03)00064-1
751

752 23. Fones H, Gurr S. The impact of Septoria tritici Blotch disease on wheat: An EU
753 perspective. Fungal Genetics and Biology. 2015;79: 3–7. doi:10.1016/j.fgb.2015.04.004
754

755 24. Torriani SF, Melichar JP, Mills C, Pain N, Sierotzki H, Courbot M. *Zymoseptoria*
756 *tritici*: A major threat to wheat production, integrated approaches to control. Fungal
757 Genetics and Biology. 2015;79: 8–12. doi:10.1016/j.fgb.2015.04.010
758

759 25. Kema GHJ, Yu D, Rijkenberg FHJ, Shaw MW, Baayen RP. Histology of the
760 pathogenesis of *Mycosphaerella graminicola* in wheat. Phytopathology. 1996;86: 777–
761 786. doi:10.1094/Phyto-86-777
762

763 26. Steinberg G. Cell biology of *Zymoseptoria tritici*: Pathogen cell organization and
764 wheat infection. Fungal Genetics and Biology. 2015;79: 17–23.
765 doi:10.1016/j.fgb.2015.04.002

766

767 27. King R, Urban M, Lauder RP, Hawkins N, Evans M, Plummer A, et al. A conserved
768 fungal glycosyltransferase facilitates pathogenesis of plants by enabling hyphal growth
769 on solid surfaces. PLoS Pathogens. 2017;13: e1006672.
770 doi:10.1371/journal.ppat.1006672

771

772 28. Motteram J, Lovegrove A, Pirie E, Marsh J, Devonshire J, van de Meene A, et al.
773 Aberrant protein N- glycosylation impacts upon infection- related growth transitions of
774 the haploid plant- pathogenic fungus *Mycosphaerella graminicola*. Molecular
775 Microbiology. 2011;81: 415–433. doi:10.1111/j.1365-2958.2011.07701.x

776

777 29. Choi YE, Goodwin SB. Gene encoding a c-Type cyclin in *Mycosphaerella*
778 *graminicola* is involved in aerial mycelium formation, filamentous growth, hyphal
779 swelling, melanin biosynthesis, stress response, and pathogenicity. Molecular Plant-
780 Microbe Interactions. 2011;24: 469–477. doi:10.1094/MPMI-04-10-0090

781

782 30. Cousin A, Mehrabi R, Guilleroux M, Dufresne M, Lee T, Waalwijk C, et al. The MAP
783 kinase- encoding gene MgFus3 of the non- appressorium phytopathogen
784 *Mycosphaerella graminicola* is required for penetration and *in vitro* pycnidia formation.
785 Molecular Plant Pathology. 2006;7: 269–278. doi:10.1111/j.1364-3703.2006.00337.x

786

787 31. Mehrabi R, M'Barek S, van der Lee TA, Waalwijk C, Wit P de, Kema GHJ. Gα and
788 Gβ proteins regulate the cyclic AMP pathway that is required for development and

789 pathogenicity of the phytopathogen *Mycosphaerella graminicola*. Eukaryotic Cell.
790 2009;8: 1001–1013. doi:10.1128/ec.00258-08
791
792 32. Mehrabi R, Kema GHJ. Protein kinase A subunits of the ascomycete pathogen
793 *Mycosphaerella graminicola* regulate asexual fructification, filamentation, melanization
794 and osmosensing. Molecular Plant Pathology. 2006;7: 565–577. doi:10.1111/j.1364-
795 3703.2006.00361.x
796
797 33. Mehrabi R, van der Lee T, Kema GHJ. MgSlt2, a cellular integrity MAP kinase gene
798 of fungal wheat pathogen *Mycosphaerella graminicola*, is dispensable for penetration
799 but essential for invasive growth. Molecular Plant-Microbe Interactions. 2006;9: 389–
800 398. doi:10.1094/MPMI-19-0389
801
802 34. Gohari AM, Mehrabi R, Robert O, Ince I, Boeren S, Schuster M, et al. Molecular
803 characterization and functional analyses of ZtWor1, a transcriptional regulator of the
804 fungal wheat pathogen *Zymoseptoria tritici*. Molecular Plant Pathology. 2014;15: 394–
805 405. doi:10.1111/mpp.12102
806
807 35. Mohammadi N, Mehrabi R, Gohari AM, Goltapeh E, Safaie N, Kema GHJ. The ZtVf1
808 transcription factor regulates development and virulence in the foliar wheat pathogen
809 *Zymoseptoria tritici*. Fungal Genetics and Biology. 2017;109: 26–35.
810 doi:10.1016/j.fgb.2017.10.003
811

812 36. Yemelin A, Brauchler A, Jacob S, Laufer J, Heck L, Foster AJ, et al. Identification of
813 factors involved in dimorphism and pathogenicity of *Zymoseptoria tritici*. PLoS ONE.
814 2017;12: e0183065. doi:10.1371/journal.pone.0183065
815
816 37. Mehrabi R, Zwiers LH, de Waard MA de, Kema GHJ. MgHog1 regulates dimorphism
817 and pathogenicity in the fungal wheat pathogen *Mycosphaerella graminicola*. Molecular
818 Plant-Microbe Interactions. 2006;19: 1262–1269. doi:10.1094/mpmi-19-1262
819
820 38. Hornby JM, Jacobitz-Kizzier SM, McNeel DJ, Jensen EC, Treves DS, Nickerson KW.
821 Inoculum size effect in dimorphic fungi: extracellular control of yeast-mycelium
822 dimorphism in *Ceratocystis ulmi*. Applied and Environmental Microbiology. 2004;70:
823 1356–9.
824
825 39. Hornby JM, Jensen EC, Lisec AD, Tasto JJ, Jahnke B, Shoemaker R, et al. Quorum
826 sensing in the dimorphic fungus *Candida albicans* is mediated by farnesol. Applied and
827 Environmental Microbiology. 2001;67: 2982–2992. doi:10.1128/AEM.67.7.2982-
828 2992.2001
829
830 40. Wedge ME, Naruzawa ES, Nigg M, Bernier L. Diversity in yeast–mycelium
831 dimorphism response of the Dutch Elm disease pathogens: the inoculum size effect.
832 Canadian Journal of Microbiology. 2016;62: 525–529. doi:10.1139/cjm-2015-0795
833
834 41. Palma-Guerrero J, Ma X, Torriani SF, Zala M, Francisco CS, Hartmann FE, et al.

835 Comparative transcriptome analyses in *Zymoseptoria tritici* reveal significant differences
836 in gene expression among strains during plant infection. Molecular Plant-Microbe
837 Interactions. 2017; doi:10.1094/MPMI-07-16-0146-R
838
839 42. Böttcher B, Pöllath C, Staib P, Hube B, Brunke S. *Candida* species rewired hyphae
840 developmental programs for chlamydospore formation. Frontiers in Microbiology.
841 2016;7: 1697. doi:10.3389/fmicb.2016.01697
842
843 43. Bago B, Zipfel W, Williams RM, Jun J, Arreola R, Lammers PJ, et al. Translocation
844 and utilization of fungal storage lipid in the arbuscular mycorrhizal symbiosis. Plant
845 Physiology. 2002;128: 108–124. doi:10.1104/pp.010466
846
847 44. Fabry W, Schmid E, Schraps M, Ansorg R. Isolation and purification of
848 chlamydospores of *Candida albicans*. Medical Mycology. 2003;41: 53–58.
849 doi:10.1080/mmy.41.1.53.58
850
851 45. Sitton JW, Cook RJ. Comparative morphology and survival of chlamydospores of
852 *Fusarium roseum* “Culmorum” and “Graminearum.” Phytopathology. 1981;71: 85–90.
853 doi:10.1094/Phyto-71-85
854
855 46. Biswas S, van Dijck P, Datta A. Environmental sensing and signal transduction
856 pathways regulating morphopathogenic determinants of *Candida albicans*. Microbiology
857 and Molecular Biology Reviews. 2007;71: 348–376. doi:10.1128/mmbr.00009-06

858

859 47. Gauthier GM. Dimorphism in fungal pathogens of mammals, plants, and insects.
860 PLoS Pathogens. 2015;11: e1004608. doi:10.1371/journal.ppat.1004608
861

862 48. Derridj S. Nutrients on the leaf surface. In : Morris CE, Nicot PC, Nguyen-The C,
863 editors. Aerial Plant Surface Microbiology. New York: Plenum Press; 1996. p. 25-42.
864

865 49. Ohm RA, Feau N, Henrissat B, Schoch CL, Horwitz BA, Barry KW, et al. Diverse
866 lifestyles and strategies of plant pathogenesis encoded in the genomes of eighteen
867 Dothideomycetes fungi. PLoS Pathogens. 2012;8: e1003037.
868 doi:10.1371/journal.ppat.1003037
869

870 50. Fleißner A, Sarkar S, Jacobson DJ, Roca GM, Read ND, Glass LN. The so locus is
871 required for vegetative cell fusion and postfertilization events in *Neurospora crassa*.
872 Eukaryotic Cell. 2005;4: 920–930. doi:10.1128/ec.4.5.920-930.2005
873

874 51. Glass NL, Rasmussen C, Roca MG, Read ND. Hyphal homing, fusion and mycelial
875 interconnectedness. Trends in Microbiology. 2004;12: 135–141.
876 doi:10.1016/j.tim.2004.01.007
877

878 52. Craven KD, Vélëz H, Cho Y, Lawrence CB, Mitchell TK. Anastomosis is required for
879 virulence of the fungal necrotroph *Alternaria brassicicola*. Eukaryotic Cell. 2008;7: 675–
880 683. doi:10.1128/ec.00423-07

881

882 53. Rosales RCP, di Pietro A. Vegetative hyphal fusion is not essential for plant infection
883 by *Fusarium oxysporum*. Eukaryotic Cell. 2008;7: 162–171. doi:10.1128/ec.00258-07
884

885 54. Shetty NP, Mehrabi R, Lütken H, Haldrup A, Kema GHJ, Collinge DB, et al. Role of
886 hydrogen peroxide during the interaction between the hemibiotrophic fungal pathogen
887 Septoria tritici and wheat. New Phytologist. 2007;174: 637–647. doi:10.1111/j.1469-
888 8137.2007.02026.x
889

890 55. Fones H, Preston GM. Reactive oxygen and oxidative stress tolerance in plant
891 pathogenic *Pseudomonas*. FEMS Microbiology Letters. 2012;327: 1–8.
892 doi:10.1111/j.1574-6968.2011.02449.x
893

894 56. Yang C, Li W, Cao J, Meng F, Yu Y, Huang J, et al. Activation of ethylene signaling
895 pathways enhances disease resistance by regulating ROS and phytoalexin production in
896 rice. The Plant Journal. 2017;89: 338–353. doi:10.1111/tpj.13388
897

898 57. Lamb C, Dixon RA. The oxidative burst in plant disease resistance. Annual Review
899 of Plant Physiology and Plant Molecular Biology. 1997;48: 251–275.
900 doi:10.1146/annurev.arplant.48.1.251
901

902 58. Nasution O, Srinivasa K, Kim M, Kim YJ, Kim W, Jeong W, et al. Hydrogen peroxide
903 induces hyphal differentiation in *Candida albicans*. Eukaryotic Cell. 2008;7: 2008–2011.

904 doi:10.1128/ec.00105-08

905

906 59. Levy E, Eyal Z, Hochmant A. Purification and characterization of a catalase-

907 peroxidase from the fungus *Septoria tritici*. Archives of Biochemistry and Biophysics.

908 1992;296: 321–327. doi:10.1016/0003-9861(92)90579-l

909

910 60. do Amaral AM, Antoniw J, Rudd JJ, Hammond-Kosack KE. Defining the predicted

911 protein secretome of the fungal wheat leaf pathogen *Mycosphaerella graminicola*. PLoS

912 ONE. 2012;7: e49904. doi:10.1371/journal.pone.0049904

913

914 61. Bignell E. The molecular basis of pH sensing, signaling, and homeostasis in fungi.

915 Advances in applied microbiology. 2012;79: 1–18. doi:10.1016/b978-0-12-394318-

916 7.00001-2

917

918 62. Ruiz-Herrera J, Leon CG, Guevara-Olvera L, Carabez-Trejo A. Yeast-mycelial

919 dimorphism of haploid and diploid strains of *Ustilago maydis*. Microbiology. 1995;141:

920 695–703. doi:10.1099/13500872-141-3-695

921

922 63. Richards A, Gow NA, Veses V. Identification of vacuole defects in fungi. Journal of

923 Microbiological Methods. 2012;91: 155–163. doi:10.1016/j.mimet.2012.08.002

924

925 64. Veses V, Gow NA. Vacuolar dynamics during the morphogenetic transition in

926 *Candida albicans*. FEMS Yeast Research. 2008;8: 1339–1348. doi:10.1111/j.1567-

927 1364.2008.00447.x

928

929 65. Edwards MC, Bowling DJF. The growth of rust germ tubes towards stomata in

930 relation to pH gradients. Physiological and Molecular Plant Pathology. 1986;29: 185–

931 196. doi:10.1016/s0048-4059(86)80020-0

932

933 66. Lendenmann MH, Croll D, Palma-Guerrero J, Stewart EL, McDonald BA. QTL

934 mapping of temperature sensitivity reveals candidate genes for thermal adaptation and

935 growth morphology in the plant pathogenic fungus *Zymoseptoria tritici*. Heredity.

936 2016;116: 384. doi:10.1038/hdy.2015.111

937

938 67. Ponomarenko A, Goodwin SB, Kema GHJ. Septoria tritici Blotch (STB) of wheat.

939 Plant Health Instructor. 2011; doi:10.1094/PHI-I-2011-0407-01

940

941 68. Nemecek JC, Wüthrich M, Klein BS. Global control of dimorphism and virulence in

942 fungi. Science. 2006;312: 583–588. doi:10.1126/science.1124105

943

944 69. Coleman M, Henricot B, Arnau J, Oliver RP. Starvation-induced genes of the tomato

945 pathogen *Cladosporium fulvum* are also induced during growth in planta. Molecular

946 Plant-Microbe Interactions. 1997;10: 1106–1109. doi:10.1094/MPMI.1997.10.9.1106

947

948 70. Talbot NJ, Ebbole DJ, Hamer JE. Identification and characterization of MPG1, a

949 gene involved in pathogenicity from the rice blast fungus *Magnaporthe grisea*. The Plant

950 Cell. 1993;5: 1575–1590. doi:10.1105/tpc.5.11.1575

951

952 71. Martin SW, Douglas LM, Konopka JB. Cell cycle dynamics and quorum sensing in
953 *Candida albicans* chlamydospores are distinct from budding and hyphal growth.
954 Eukaryotic Cell. 2005;4: 1191–1202. doi:10.1128/ec.4.7.1191-1202.2005

955

956 72. Oliveira RR, Aguiar BM, Tessmann DJ, Pujade-Renaud V, Vida JB. Chlamydospore
957 formation by *Corynespora cassiicola*. Tropical Plant Pathology. 2012;37: 415–418.
958 doi:10.1590/s1982-56762012000600006

959

960 73. Annone JG. Observacion de conidios secundarios de *Septoria tritici* Rob. ex Desm.
961 por meio de impresiones foliareas. In : Kohli MM, van Beuningen LT, editors. In :
962 Conferencia regional sobre la septoriosis del trigo. Centro International de Mejoramiento
963 de Maiz y Trigo (CIMMYT). Montevideo, 1990. p. 80-87.

964

965 74. Djerbi M. Épidémiologie du *Septoria tritici* Rob. et Desm. consevation et mode de
966 formation de l'inoculum primaire. Société Française de Phytopathologie. 1977; 91–101.

967

968 75. Jones GD, Lee NP. Production of secondary conidia by *Septoria tritici* in culture.
969 Transactions of the British Mycological Society. 1974;62: 212-213. doi:10.1016/s0007-
970 1536(74)80025-2

971

972 76. Zhan J, Linde CC, Jürgens T, Merz U, Steinebrunner F, McDonald BA. Variation for

973 neutral markers is correlated with variation for quantitative traits in the plant pathogenic
974 fungus *Mycosphaerella graminicola*. Molecular Ecology. 2005;14: 2683–2693.
975 doi:10.1111/j.1365-294x.2005.02638.x
976
977 77. Croll D, Zala M, McDonald BA. Breakage-fusion-bridge cycles and large insertions
978 contribute to the rapid evolution of accessory chromosomes in a fungal pathogen. PLoS
979 Genetics. 2013;9: e1003567. doi:10.1371/journal.pgen.1003567
980
981 78. Kilaru S, Schuster M, Studholme D, Soanes D, Lin C, Talbot NJ, Steinberg G. A
982 codon-optimazed green fluorescent protein for live cell imaging in *Zymoseptoria tritici*.
983 Fungal Genetics and Biology. 2015;79: 125–131.
984
985 79. Zala M, Mikaberidze A, Alassimone JPL, Muhammad A, McDonald BA, Sánchez-
986 Vallet A. Mixed infections alter virulence dynamics and reduce transmission in the wheat
987 pathogen *Zymoseptoria tritici*. in submission.
988
989 80. Vogel HJ. A convenient growth medium for Neurospora (medium N). Microbial
990 Genetics Bulletin. 1956;13: 42–43.
991
992 81. Bolger AM, Lohse M, Usadel B. Trimmomatic: a flexible trimmer for Illumina
993 sequence data. Bioinformatics. 2014;30: 2114–2120. doi:10.1093/bioinformatics/btu170
994
995 82. Trapnell C, Pachter L, Salzberg SL. TopHat: discovering splice junctions with RNA-

Seq. Bioinformatics. 2009;25: 1105–1111. doi:10.1093/bioinformatics/btp120

83. Anders S, Pyl PT, Huber W. HTSeq—a Python framework to work with high-throughput sequencing data. Bioinformatics. 2015;31: 166–169. doi:10.1093/bioinformatics/btu638

84. Robinson MD, Oshlack A. A scaling normalization method for differential expression analysis of RNA-seq data. Genome Biology. 2010;11: 1–9. doi:10.1186/gb-2010-11-3-r25

85. Robinson MD, McCarthy DJ, Smyth GK. edgeR: a Bioconductor package for differential expression analysis of digital gene expression data. Bioinformatics. 2010;26: 139–140. doi:10.1093/bioinformatics/btp616

86. Grandaubert J, Bhattacharyya A, Stukenbrock EH. RNA-seq based gene annotation and comparative genomics of four fungal grass pathogens in the genus *Zymoseptoria* identify novel orphan genes and species-specific invasions of transposable elements. G3: Genes|Genomes|Genetics. 2015;5: 1323–1333. doi:10.1534/g3.115.017731

87. Plissonneau C, Hartmann FE, Croll D. Pangenome analyses of the wheat pathogen *Zymoseptoria tritici* reveal the structural basis of a highly plastic eukaryotic genome. BMC Biology. 2018;16: 5. doi:10.1186/s12915-017-0457-4

1019 88. Wickham H. ggplot2 – Elegant Graphics for Data Analysis . 2nd ed. Springer-Verlag;
1020 2009. p. 260. doi:10.18637/jss.v077.b02
1021
1022 89. Meile L, Croll D, Brunner PC, Plissonneau C, Hartmann FE, McDonald BA, et al. A
1023 fungal avirulence factor encoded in a highly plastic genomic region triggers partial
1024 resistance to Septoria tritici Blotch. New Phytologist. 2018;219: 1048–1061.
1025 doi:10.1111/nph.15180
1026
1027

1028 Supporting information

1029

1030 **S1 Fig. Effect of nitrogen depletion stress on the cell morphology of four**
1031 ***Zymoseptoria tritici* strains.** A nutrient-poor medium (MM without ammonium nitrate)
1032 was used to monitor the growth form transition. (A) At 24 hai, only blastospores from the
1033 1E4 strain switched to hyphal growth forming lateral filaments (black arrow). The rest of
1034 the strains remain undifferentiated. Bars represent 10 μm. (B) At 72 hai, blastospores of
1035 all tested *Z. tritici* strains incubated under nitrogen depletion undergo a blastospore-to-
1036 hyphae transition. Branching and hyphal elongation were predominantly observed at this
1037 time point. Bars represent 30 μm. (C) Regular MM containing ammonium nitrate induced
1038 a mixture of morphotypes, such as blastospores, hyphae and budding blastospores from
1039 filamentous hyphae. Bars represent 30 μm.
1040

1041 **S2 Fig. Effect of exogenous oxidative stress induced by H_2O_2 on the cell**
1042 **morphology of four *Zymoseptoria tritici* strains using a high blastospore inoculum**
1043 **density (10^5 blastospore/mL).** A nutrient-rich medium (YSB) containing different
1044 concentrations of H_2O_2 was used to incubate the strains under oxidative stress for 72
1045 hours. Blastopores kept on YSB medium without addition of H_2O_2 continue to multiply as
1046 budding blastospores via blastosporulation and were used as a control (A, B, C, D - bars
1047 represent 50 μm). Despite the increases in H_2O_2 concentration in the medium, no
1048 morphological changes were observed for 1A5 (E, I, M, Q – bars represent 50 μm), 3D1
1049 (G, K – bars represent 50 μm; O and S – bars represent 10 μm), and 3D7 (H, L, P, T -
1050 bars represent 50 μm). The 1E4 strain responded morphologically to H_2O_2 concentrations
1051 at 0.5 mM, 1 mM, and 5 mM (F, J, N - bars represent 50 μm) undergoing the blastospore-
1052 to-hyphae transition. As observed for other strains (Q, S, and T), blastospores of the 1E4
1053 strain remained as undifferentiated structures at 10 mM (R - bars represent 50 μm).
1054
1055 **S3 Fig. Effect of exogenous oxidative stress induced by H_2O_2 on the cell**
1056 **morphology of four *Zymoseptoria tritici* strains using a low blastospore inoculum**
1057 **density (10^3 blastospore/mL).** A nutrient-rich medium (YSB) containing different
1058 concentrations of H_2O_2 was used to incubate the strains under oxidative stress for 96
1059 hours. Blastopores kept on YSB medium without addition of H_2O_2 continued to multiply as
1060 budding blastospores via blastosporulation and were used as a control. At 0.5 mM, only
1061 the 1E4 and 3D1 strains showed hyphal branching and the initial formation of mycelium.
1062 At 1 mM, blastospores from 1E4, 3D1, and 3D7 grew as a mixture of pseudohyphae

1063 (asterisks) and filamentous hyphae (black arrows). At 2 mM, none of the strains changed
1064 their morphology nor were they able to asexually reproduce via blastosporulation.
1065 Blastospores of the 1A5 strain did not switch to different morphotypes in any of the tested
1066 concentrations of H_2O_2. Bars represent 10 μm.
1067
1068 **S4 Fig. Cell morphology of four *Zymoseptoria tritici* strains after 144 hours of**
1069 **incubation on two distinct hyphal induction media and at different initial cell**
1070 **densities.** (A) Blastospores incubated in carbon-depleted MM at 18°C demonstrated a
1071 morphological independence of the inoculum size until the concentration of 10^5
1072 blastospores/mL, where they were able to switch to hyphal growth and to form mycelial
1073 colonies. At higher initial inoculum concentrations ($\geq 10^6$ blastospores/mL), a drastic
1074 reduction of growth form transition and in hyphal length was observed for all tested strains.
1075 (B) Blastospores incubated in YSB medium at 27°C showed significant differences among
1076 the strains. At lower initial inoculum concentrations (10^3 and 10^4 blastospores/mL) only
1077 pseudohyphae and chlamydospores formed. Intermediate inoculum concentrations (10^5
1078 blastospores/mL and 10^6 blastospores/mL) promoted hyphal growth for the 1E4, 3D1 and
1079 3D7 strains. A ten-fold increase in the initial cell density (10^7 blastospores/mL) favored
1080 chlamydospore formation in all strains. 1A5 blastospores were not able to switch to
1081 hyphae and undergo transitions to pseudohyphae and chlamydospores for all tested
1082 concentrations. Bars represent 10 μm.
1083

1084 **S5 Fig. Morphological forms of four *Zymoseptoria tritici* strains grown in two**
1085 **distinct morphotype-induction conditions used for the RNA-Seq.** Nutrient-rich
1086 medium (YSB) induces only blastosporulation. Nutrient-poor medium (MM) and the wheat
1087 leaf surface induced the blastospore-to-hyphae transition and mycelial growth in all tested
1088 strains. Wheat leaves infected with *Z. tritici* strains expressing cytoplasmic GFP (green
1089 color) were analyzed using confocal microscopy. The blue color corresponds to
1090 chlorophyll A detected from chloroplast autofluorescence. Bars represent 10 μm.
1091
1092 **S6 Fig. Core transcriptome signatures of four *Zymoseptoria tritici* strains from two**
1093 **distinct growth phases.** (A-B) Venn diagram of the overexpressed genes (FDR≤0.01)
1094 for each strain grown under blastospore and mycelial growth conditions. (C) Graphic
1095 representing average expression (log2-transformed counts per million values) of seven
1096 genes related to blastosporulation during the blastospore growth phase among strains.
1097 (D) Graphic representing average expression (log2-transformed counts per million values)
1098 of 38 virulence-related genes during the mycelial growth phase. (E) Graphic representing
1099 average expression (log2-transformed counts per million values) of six genes related to
1100 cellular morphogenesis during the mycelial growth phase.
1101
1102 **S7 Fig. Chlamydospore cells observed in a spore solution harvested from 20-day-**
1103 **old infected leaves.** Plants were previously inoculated with pycnidiospores of four *Z. tritici*
1104 strains. Free chlamydospores expressing cytoplasmic GFP were frequently observed

1105 mixed with pycnidiospores in the spore solution of all tested strains. Bars represent 30
1106 µm. The proportion of chlamydospores was visibly lower compared to pycnidiospores.
1107
1108 **S1 Table.** Overview of the transcriptomic data of four *Zymoseptoria tritici* strains obtained
1109 from two distinct growth phases (blastospore *vs.* mycelium).
1110
1111 **S2 Table.** The shared 134 genes overexpressed during blastospore growth phase among
1112 four *Zymoseptoria tritici* strains.
1113
1114 **S3 Table.** The shared 134 genes overexpressed during mycelial growth phase among
1115 four *Zymoseptoria tritici* strains.
1116
1117 **S4 Table.** Expression values of seven genes overexpressed in blastospore growth phase
1118 and associated with blastosporulation.
1119
1120 **S5 Table.** Expression values of 39 genes overexpressed in mycelium growth phase and
1121 associated with virulence factors.
1122
1123 **S6 Table.** Expression values of six genes overexpressed in mycelium growth phase and
1124 associated with cellular morphogenesis.
1125
1126

1127 ## Figures and Tables

1128

1129 **Figure Captions**

1130 **Fig 1. Effect of temperature on the cell morphology of four *Zymoseptoria tritici***
1131 **strains.** (A) Blastospores incubated on nutrient-rich YSB medium at 18°C (the control
1132 environment) multiply by budding as blastospores (white triangles). (B) The effect of high
1133 temperatures on *Z. tritici* morphology was observed by exposing the strains to 27°C. At 8
1134 hours after incubation (hai) at the high temperature, blastospores of the 1E4 strain were
1135 faster to respond to the new environment by switching to filamentous growth. Black
1136 triangles point to hyphal branches. (C) At 24 hai, blastospores of the 3D1 and 3D7 strains
1137 began growing as hyphae. The 1A5 strain produced swollen cells (black arrows) and
1138 pseudohyphae (asterisks), without any evidence of hyphal differentiation. (D) At 48 hai,
1139 hyphal branches were abundant for the 1E4, 3D1, and 3D7 strains. The 1A5 strain
1140 continued to produce only swollen structures (black arrows). (E) At 96 hai, filamentous
1141 growth was observed for the 1E4, 3D1, and 3D7 strains. For the 1A5 strain, high
1142 temperature promoted the formation of two new morphotypes: pseudohyphae (asterisks)
1143 and chlamydospore-like cells (black arrows). (F) After 144 hours of incubation, the
1144 formation of chlamydospore-like cells was observed mainly at the tips of pseudohyphae
1145 for the 1A5 strain and at the distal ends of mycelial filaments for the remaining strains
1146 (1E4, 3D1, and 3D7) (black arrows). Bars represent 10 μm.

1147

1148 **Fig 2. Effect of carbon limitation on the cell morphology of four *Zymoseptoria tritici***
1149 **strains.** A nutrient-rich medium (YSB) and a carbon-depleted medium (Minimal Media
1150 without sucrose) were used to monitor the growth form transitions. (A) Blastospores
1151 incubated on YSB continued to multiply as budding blastospores and were used as
1152 controls. (B) Under carbon limitation stress, the blastospores of all tested strains began
1153 growing as hyphae after 24 hours of incubation (arrows). (C) At 144 hai, a mycelial growth
1154 was predominant, with frequent vegetative cell fusion events (asterisks) among hyphae.
1155 Bars represent 20 µm.
1156
1157 **Fig 3. Transcriptome signatures of blastospore and mycelial growth phases**
1158 **organized based on enrichment of molecular functional terms.** (A) Common
1159 upregulated genes during blastospore growth among the *Zymoseptoria tritici* strains. (B)
1160 Common upregulated genes for mycelial growth among the *Z. tritici* strains.
1161
1162 **Fig 4. Staining of cell wall chitin and lipid content in the different morphotypes of**
1163 ***Zymoseptoria tritici.*** Cell walls were stained with the chitin-binding dye Calcofluor White
1164 (blue color) and the lipid droplets were stained with Nile Red (red color). Blastospores,
1165 hyphae, and pseudohyphae showed a weaker fluorescence for Calcofluor White
1166 compared to chlamydospores (A), including those formed terminally (B) or intercalarily (C)
1167 via suspensor cells. A high accumulation of lipid droplets was observed in
1168 chlamydospores, as well as in blastospores and pseudohyphae. Hyphae only showed a
1169 high accumulation of lipid droplets in the hyphal branching zone. Bars represent 10 μm.

1170

1171 **Fig 5. Chlamydospore cells produced by *Zymoseptoria tritici* have thicker cell walls**
1172 **than pycnidiospores and blastospores.** Black triangles point to a detaching daughter
1173 cell budding from a blastospore mother cell. Images were obtained by transmission
1174 electron microscopy. Two different magnifications are shown for each morphotype: upper
1175 panel scale bar = 2000 nm (low magnification), lower panel scale bar = 500 nm (high
1176 magnification).

1177

1178 **Fig 6. Chlamydospores produced by *Zymoseptoria tritici* are able to germinate both**
1179 ***in vitro* and on the surface of wheat leaves.** (A) Blastospores were used as a control.
1180 Apical germination and hyphal elongation were observed after 12 hours of incubation on
1181 water agar (WA) plates at 18°C. At 24 hai, blastosporulation was observed from the
1182 germinated blastospores. (B) Terminal chlamydospores formed via suspensor cells and
1183 (C) free-chlamydospores began to germinate after 12 h of incubation on water agar.
1184 Hyphal elongation was obvious by 24 h. Bars represent 10 μm. (D) Free-chlamydospores
1185 (upper image) and terminal chlamydospores (lower image) expressing GFP (green color)
1186 produced germ tubes on the surface of wheat leaves at 24 hours after infection. Blue color
1187 corresponds to the autofluorescence detected from chlorophyll A. Asterisks indicate the
1188 suspensor cells where chlamydospores are attached. Bars represent 8 μm.

1189

1190 **Fig 7. Chlamydospores produced by *Zymoseptoria tritici* are more tolerant to stress**
1191 **than blastospores and pseudohyphae.** Survival rate (%) was estimated based upon

1192 the number of colonies formed after exposure to the stressful environment compared to
1193 the number of colonies formed in the control environment after seven days. (A)
1194 Blastospores, pseudohyphae and chlamydospore cells were kept for 1, 3, 5, and 10 days
1195 in a sealed box containing anhydrous silica gel to produce a dry environment. This
1196 simulated drought stress affected blastospore and pseudohyphae survival over time.
1197 Chlamydospores were less affected and exhibited a survival rate of 50% after 10 days
1198 under drought stress. (B) The same three morphotypes were subjected to a cold shock.
1199 Blastospores, pseudohyphae, and chlamydospores were submerged in liquid nitrogen for
1200 1, 2, and 3 minutes at -196 °C. Only chlamydospores survived this cold stress. (C) The
1201 same three morphotypes were subjected to heat stress based on incubation for 24 hours
1202 at 30°C, 35°C or 40°C. Blastospores and chlamydospores were equally affected at 30°C.
1203 The incubation at 35°C killed all the blastospores, while chlamydospore survived at a 12%
1204 rate, double the rate observed for pseudohyphae (6%). No colonies were observed after
1205 incubation at 40°C. One star indicates that the adjusted p value is less than 0.05, two
1206 stars indicates that the p value is less than 0.005, and three stars indicates that the p
1207 value is less than 0.0005. ns indicates no significant difference.

1208

1209 **Fig 8. Germinated pycnidiospores of *Zymoseptoria tritici* produce new**
1210 **blastospores via blastosporulation on the surface of wheat leaves.** (A) At 24 hours
1211 after infection, pycnidiospores (asterisk) germinated and formed hyphal branches
1212 expressing GFP (green color). The germinated pycnidiospores produced new
1213 blastospores on the host leaves (arrow). (B) We observed a significant increase in budding

1214 points on germinated pycnidiospores (arrows), as well as more free blastospores on the
1215 leaf surface at 48 hours after infection. At this time point, we also observed several
1216 vegetative cell fusion events between blastospores and pycnidiospores, which are
1217 characterized by a tubular shaped bridge between the fusing cells (asterisks). Blue color
1218 corresponds to autofluorescence detected from chlorophyll A. Bars represent 10 μm.
1219

1220 ## Accession numbers

1221 All raw sequencing data were deposited into the NCBI Sequence Read Archive under the
1222 accession number SRP152081.
1223

1224 ## Author contributions

1225 **Conceptualization:** Carolina Sardinha Francisco, Javier Palma-Guerrero
1226 **Formal analysis:** Carolina Sardinha Francisco, Xin Ma, Javier Palma-Guerrero.
1227 **Funding acquisition:** Bruce A. McDonald
1228 **Investigation:** Carolina Sardinha Francisco, Maria Manuela Zwyssig, Javier Palma-
1229 Guerrero.
1230 **Methodology:** Carolina Sardinha Francisco, Javier Palma-Guerrero.
1231 **Project administration:** Javier Palma-Guerrero
1232 **Resources:** Bruce A. McDonald
1233 **Supervision:** Javier Palma-Guerrero, Bruce A. McDonald
1234 **Validation:** Carolina Sardinha Francisco

Writing – original draft: Carolina Sardinha Francisco, Javier Palma-Guerrero, Bruce A. McDonald.

Writing – review & editing: Carolina Sardinha Francisco, Javier Palma-Guerrero, Bruce A. McDonald.

Financial disclosure statement

C.S.F. was supported by a PhD research fellowship from CAPES - Brazil (process n° 002087/2015-04). The funders had no role in study design, data collection and analysis, decision to publish, or preparation of the manuscript.

Competing interests

The authors have declared that no competing interests exist.

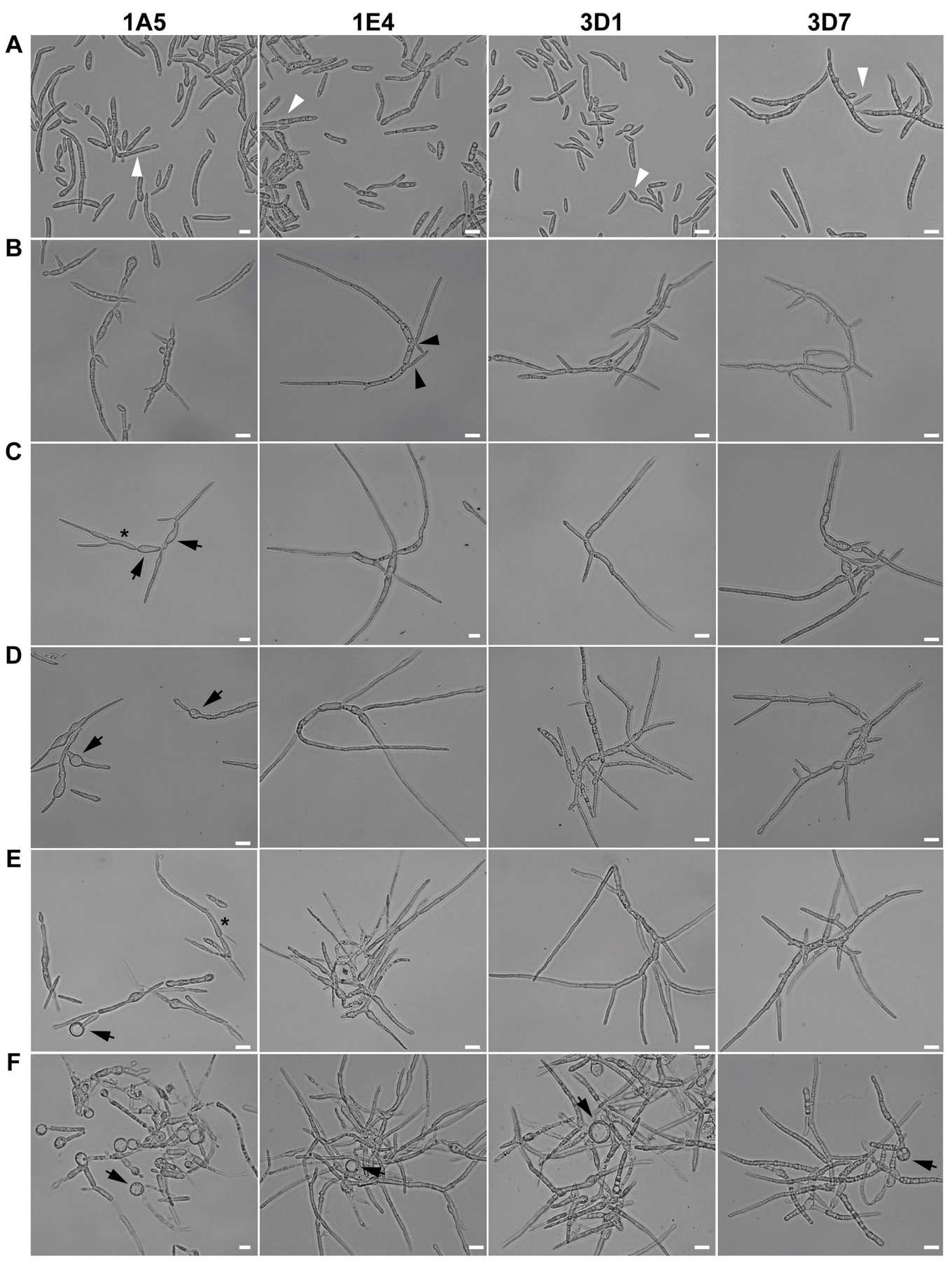
1A5
1E4
3D1
3D7
A
B
C
D
E
F

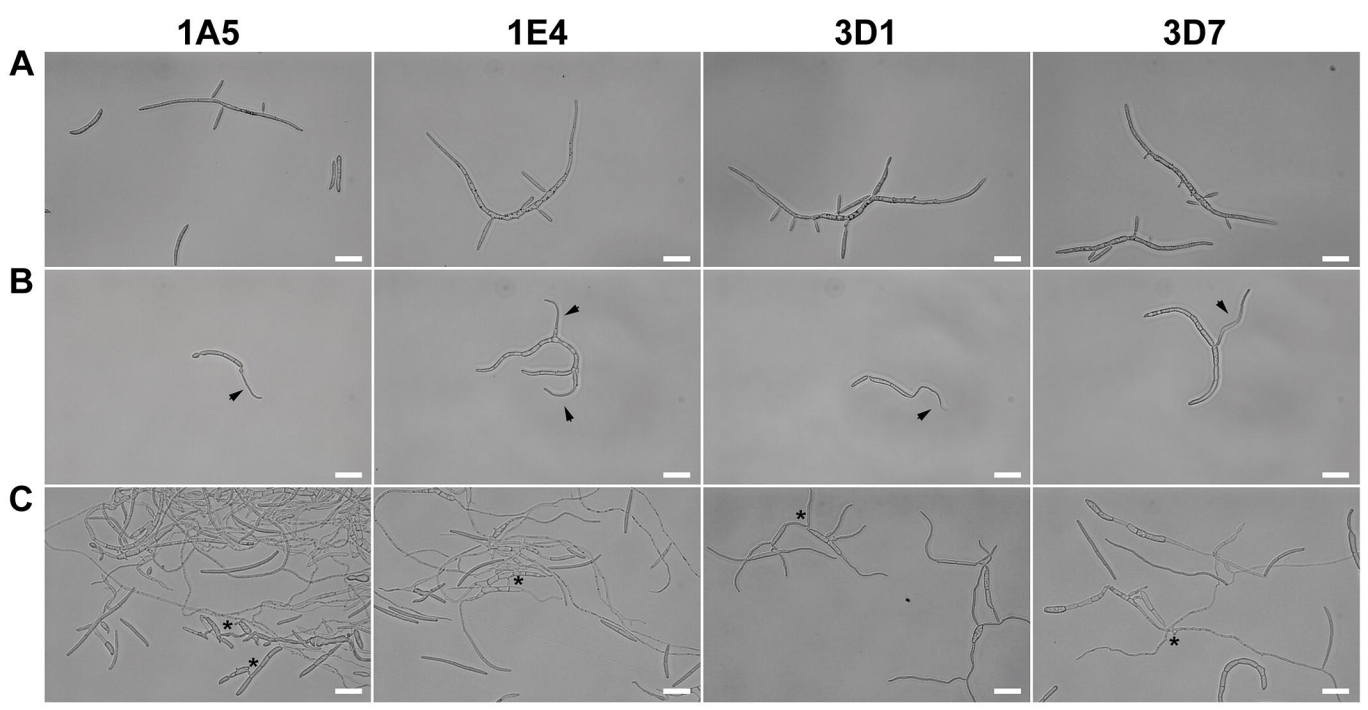
1A5
1E4
3D1
3D7
A
B
C

A Upregulated genes during blastospore growth

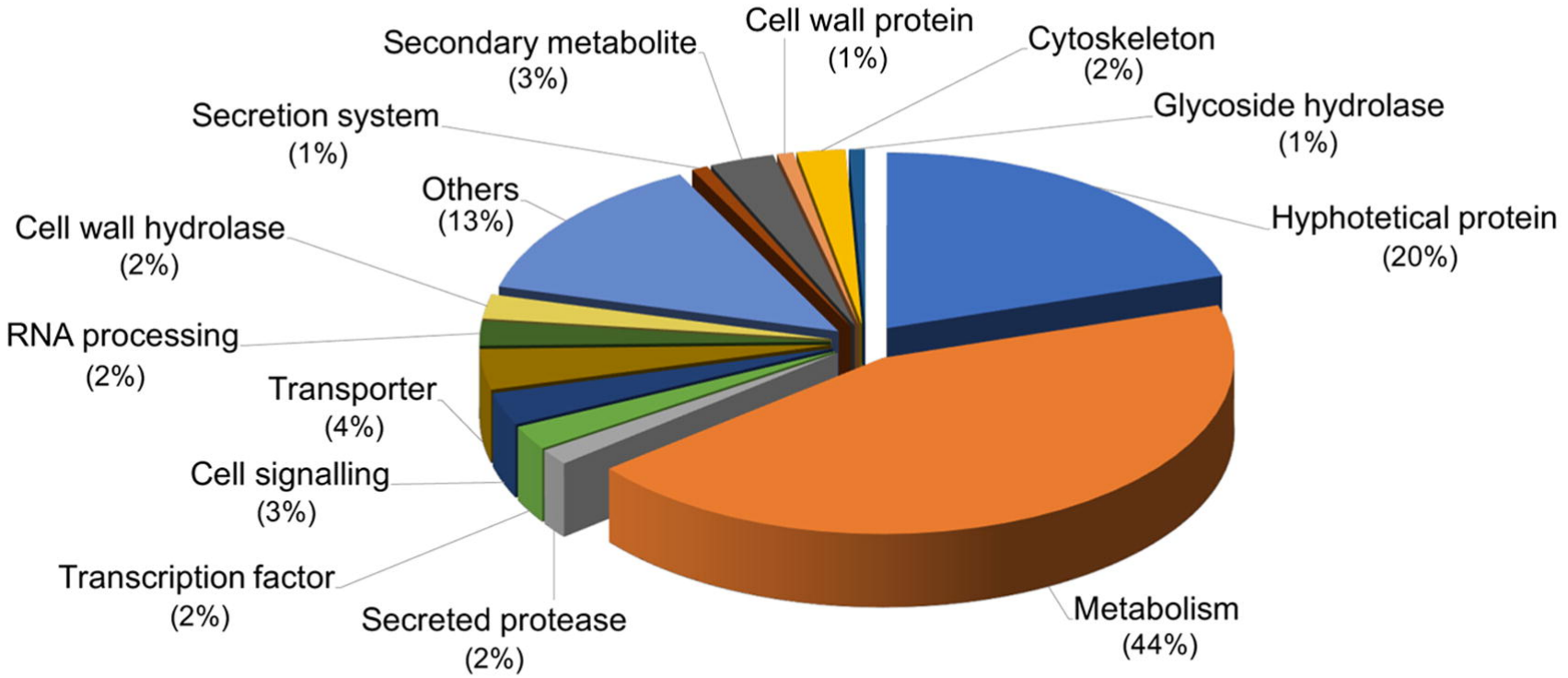

B Upregulated genes during hyphal growth

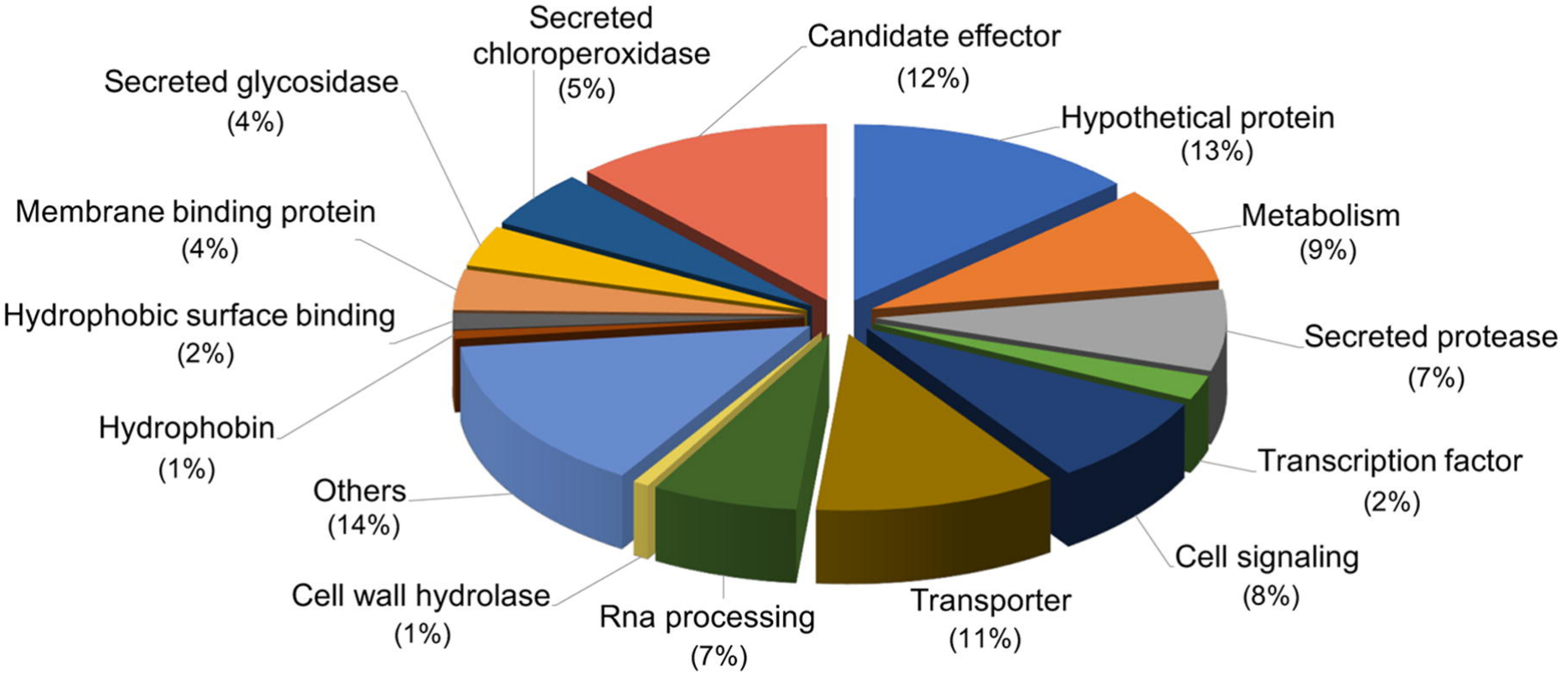

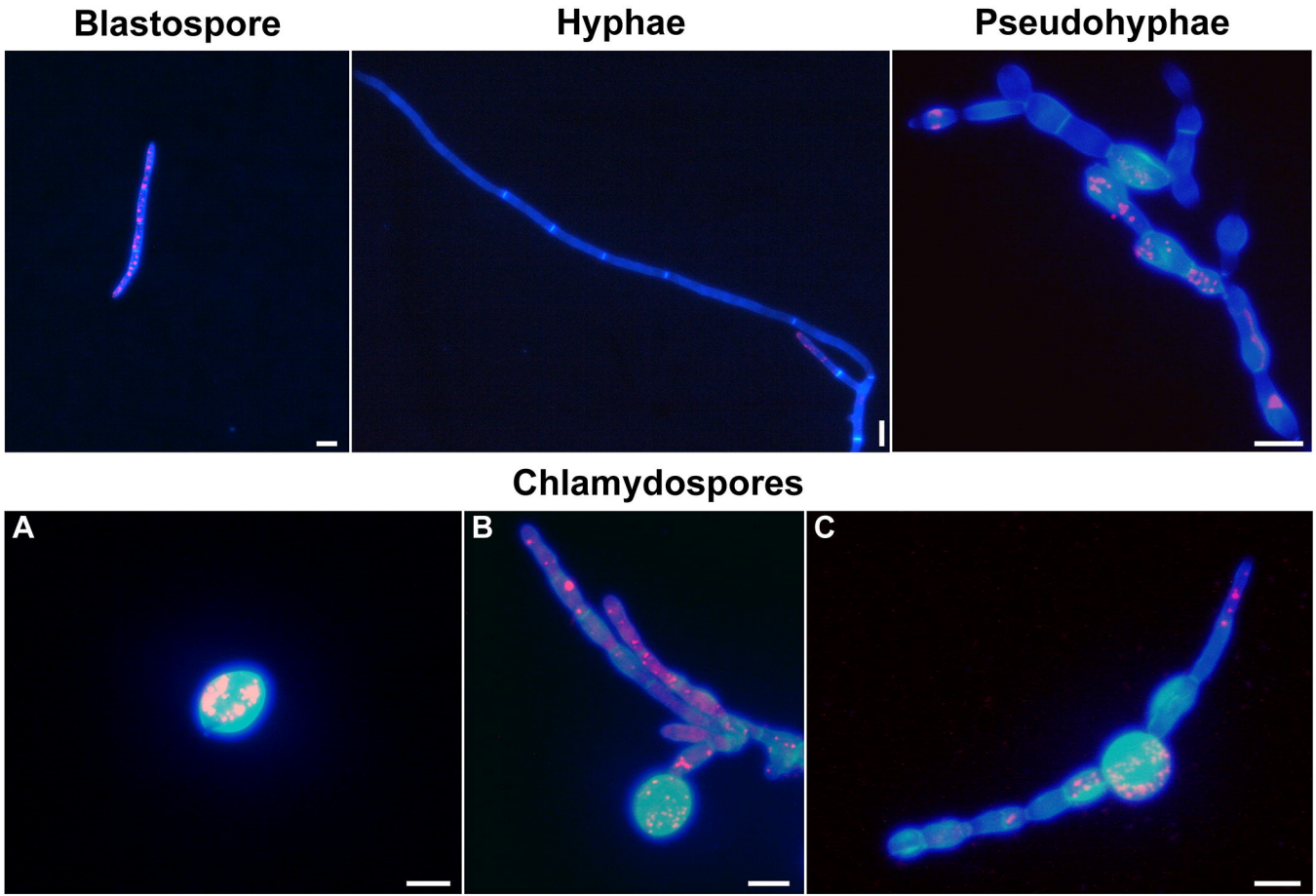
Blastospore
Hyphae
Pseudohyphae
Chlamydospores
A
B
C

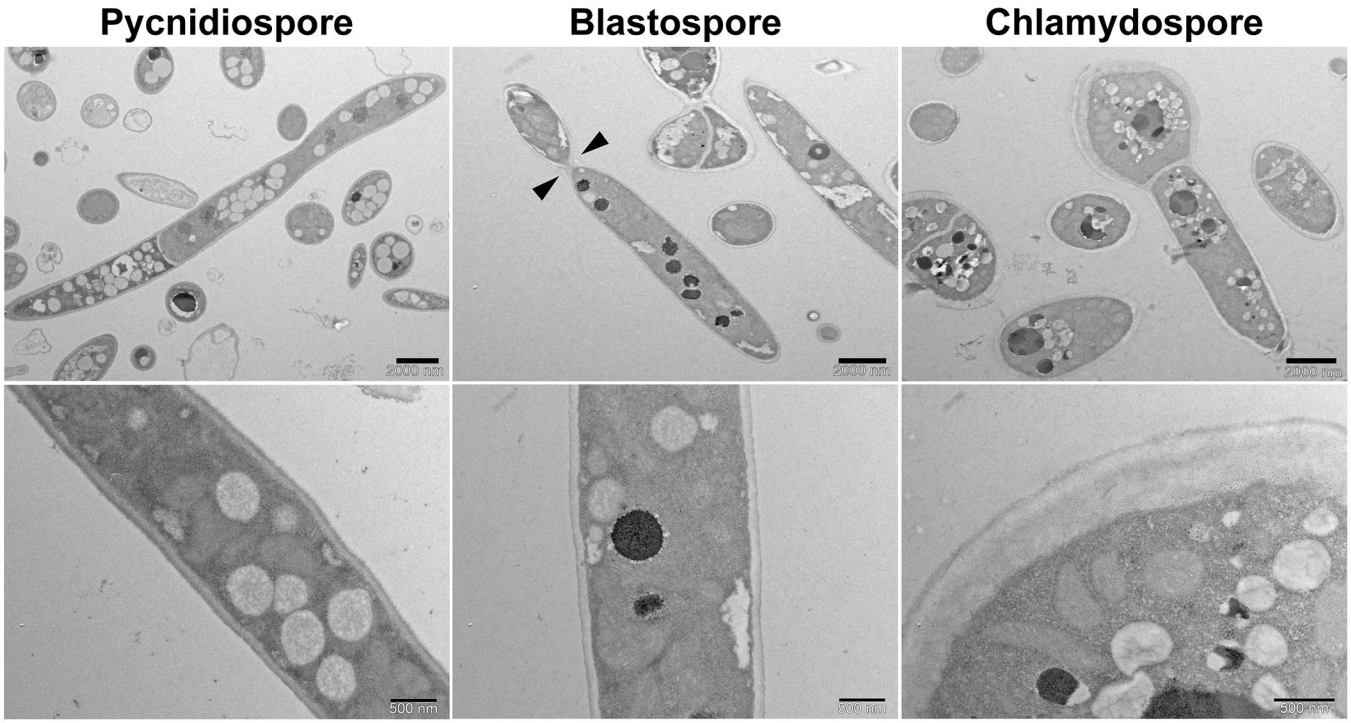
Pycnidiospore
Blastospore
Chlamydospore
2000 nm
2000 nm
2000 nm
500 nm
500 nm
500 nm

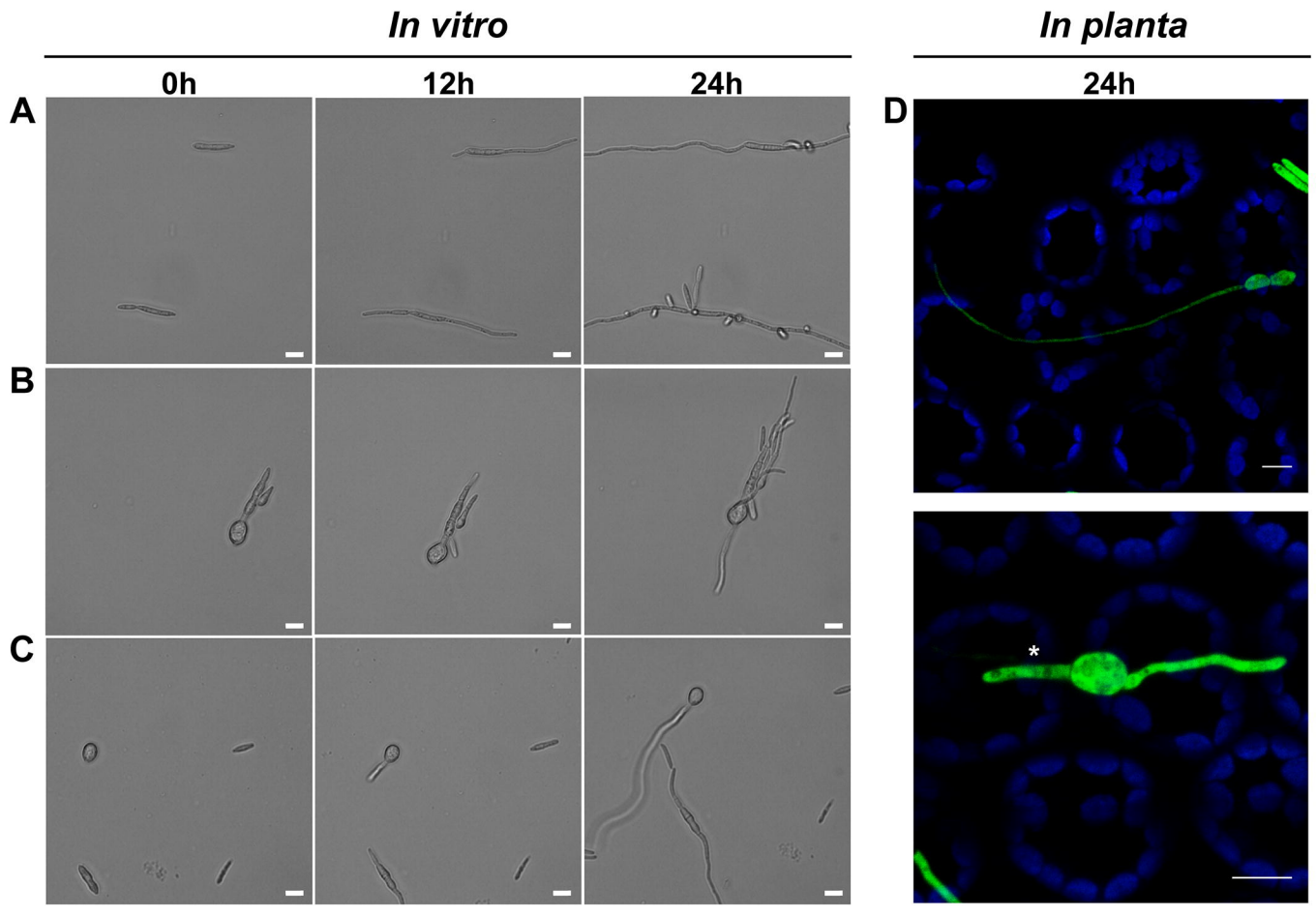
In vitro
In planta
0h
12h
24h
24h
A
B
C
D
*

A
Drought
B
Cold stress
C
Heat stress
Survival rate (%)
100
75
50
25
0
1d
3d
5d
10d
1min
2min
3min
30°C
35°C
40°C
Chlamydospore
Blastospore
Pseudohyphae
**
*
***
NS

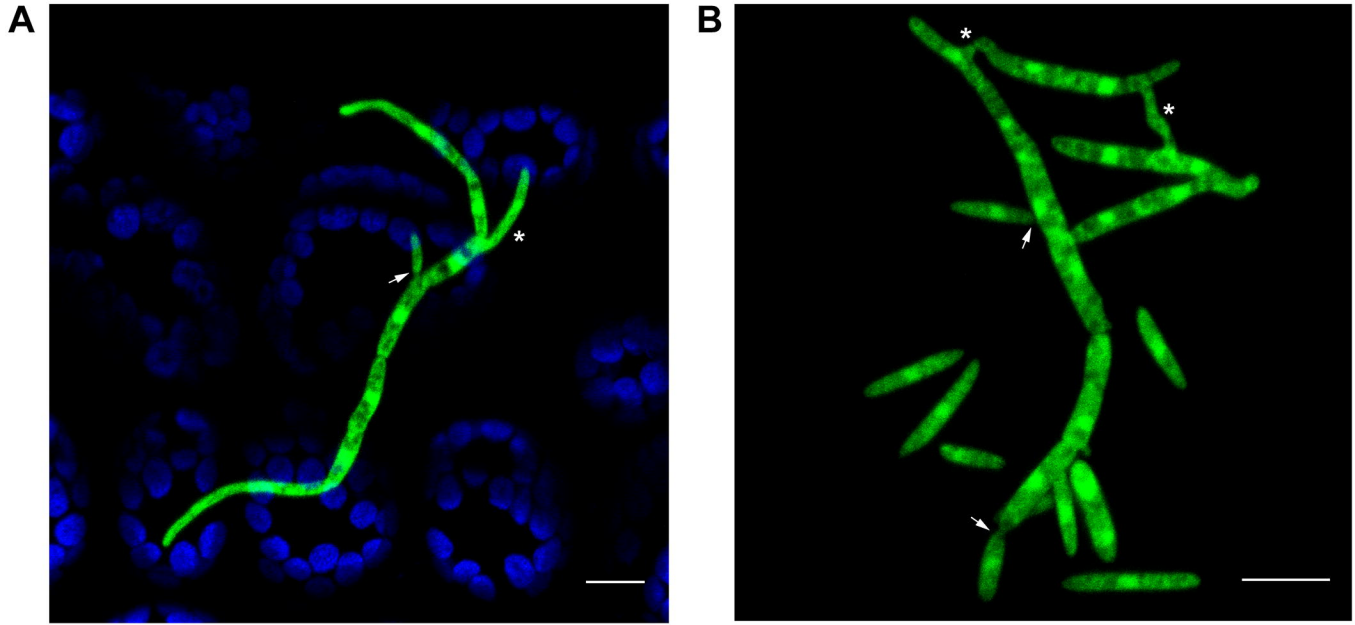
A
B